İSTANBUL TECHNICAL UNIVERSITY ★ INSTITUTE OF SCIENCE AND TECHNOLOGY

USING CNN BASED ANTENNAL LOBE MODEL TO ACCELERATE ODOR CLASSIFICATION

M.Sc. Thesis by
Tuba AYHAN, M.Sc.

Department : **Electronics and Communication Engineering**

Programme : **Electronics Engineering Engineering**

Thesis Supervisor: Doç. Dr. Müştak Erhan YALÇIN

JUNE 2010

İSTANBUL TECHNICAL UNIVERSITY ★ INSTITUTE OF SCIENCE AND TECHNOLOGY

USING CNN BASED ANTENNAL LOBE MODEL TO ACCELERATE ODOR CLASSIFICATION

M.Sc. Thesis by
Tuba Ayhan
(504081226)

Date of submission : **07 May 2010**
Date of defence examination: **10 June 2010**

Supervisor (Chairman) : **Doç. Dr. Müştak Erhan YALÇIN (ITU)**
Members of the Examining Committee : **Doç. Dr. Neslihan Şengör (İTÜ)**
Yrd. Doç.Dr. Mustafa Ersel Kamaşak (İTÜ)

JUNE 2010

İSTANBUL TEKNİK ÜNİVERSİTESİ ★ FEN BİLİMLERİ ENSTİTÜSÜ

KOKULARIN SINIFLANDIRILMASININ HIZLANDIRILMASI İÇİN HYSA TABANLI ANTENAL LOBE MODELİ KULLANIMI

YÜKSEK LİSANS TEZİ
Tuba AYHAN
(504081226)

Tezin Enstitüye Verildiği Tarih : 07 Mayıs 2010
Tezin Savunulduğu Tarih : 10 Haziran 2010

Tez Danışmanı : Doç. Dr. Müştak Erhan YALÇIN (ITU)
Diğer Jüri Üyeleri : Doç. Dr. Neslihan Şengör (İTÜ)
Yrd. Doç.Dr. Mustafa Ersel Kamaşak (İTÜ)

Haziran 2010

FOREWORD

I would like to thank my supervisor Müştak E. Yalçın who has supported me during my master and leaded me to collaborate with Biocircuits Institute, UCSD. I am very grateful to M. Kerem Müezzinoğlu for his great technical support and guidance. I also acknowledge the support from TUBİTAK BİDEB-2210 during my master study.

This work is supported by Istanbul Technical University under master thesis support program.

May 2010

Tuba Ayhan

Electronics Engineer

TABLE OF CONTENTS

Page

ABBREVIATIONS

1-NN **:** 1 Nearest Neighborhood
ANN **:** Artificial Neural Network
CDA : Canonical Discriminant Analysis
CNN **:** Cellular Neural/Nonlinear Network
CPL **:** Characteristic Path Length
FW **:** Feature Weighting
k-NN **:** k Nearest Neighborhood
MB **:** Mushroom Body
MI **:** Mutual Information
NBC **:** Naive Bayes Classifier
OBP **:** Odor Binding Protein
OR **:** Olfactory Receptor
PCA **:** Principle Component Analysis
ppm **:** Parts per million
RBF **:** Radial Basis Function
SVM **:** Support Vector Machine
SWCNN **:** Small World Cellular Neural/Nonlinear Network

LIST OF TABLES

Page

LIST OF FIGURES

Page

USING CNN BASED ANTENNAL LOBE MODEL TO ACCELERATE ODORCLASSIFICATION

SUMMARY

Like classifying audio and visual signals, odor information collected by a sensor array can also be classified according to their densities or species and processed in order to be used in applications such as security, improving food quality and medical requirements. However, the working principle of odor detecting sensors requires additional processing in sensor response evaluation

Electronic noses are used to detect and process odors and metal oxide gas sensor are widely used for detection. For metal oxide gas sensors, to settle on a stable value may take long time of minutes order. Timing is not an issue in most of the previous research, so classification on transient regime of the sensor response was not deeply considered.

In addition, invested the biological olfaction system, time required for a odor receptor is around 100ms where time needed for decision is around 40ms. This fact tells the importance of the key role that *antennal lobe* in insects and *olfactive bulb* in vertebrates play.

In this thesis, antennal lobe is modeled by cellular neural network (CNN) in three different topologies to accelerate the odor classification and these models are tested with different scenarios (data set and classifier). All the models employ two types of neurons opposite to usual CNN. One of the models has one layer with local couplings, one has two layers and the other has two layers built with small world phonemenon. Moreover, effect of sensor temperature on classification performance for different features and classifiers is investigated.

KOKULARIN SINIFLANDIRILMASININ HIZLANDIRILMASI İÇİN HYSA TABANLI ANTENAL LOBE MODELİ KULLANIMI

ÖZET

Ses ve görüntü işaretlerinin sınıflandırılması gibi, bir sensör dizisi tarafından toplanan koku işareti de, güvenlik, gıda kalitesinin arttırılması, tıbbi gereklilikler ve benzeri amaçlara hizmet etmek için işlenebilir; kokular türlerine ve yoğunluklarına göre sınıflandırılabilir. Ancak kokuyu algılamak için kullanılan sensörlerin çalışma karakteristiği, sensör cevabının işlenmesinde ek tekniklere başvurulmasını zorunlu kılar.

Kokuları sezmek ve işlemek için geliştirilen *elektronik burun*larda sıkça kullanılan bir sensör cinsi olan metal oksit gaz sensörlerinin sabit bir çıkış değerine ulaşmaları dakikalar mertebesinde sürebilmektedir. Şimdiye kadar yapılan çalışmaların çoğunda hız önemli bir ölçüt olmadığından, sensör cevabının geçici rejiminde sınıflama işlemi üzerinde fazla durulmamıştır.

Öte yandan biyolojik koku alma sistemlerine baktığımızda, koku alma reseptörlerinin sabit bir potansiyele oturması 100ms sürmekteyken, sınıflama işleminin 40ms içinde bitmesi bize koku reseptörlerinin cevabını geçici rejimde işleyen böceklerde *antenal lob*, omurgalılarda *olfaktif bulb* organlarının önemini göstermektedir.

Bu tezde, koku sınıflandırma işleminin hızlandırılabilmesi için antenal lob hücresel yapay sinir ağı (HYSA) kullanılarak üç farklı topolojide modellenmiş, farklı senaryolarla (veri kümesi ve sınıflayıcı) test edilmiştir. Tüm modeller alışılmış bir HYSA'nın aksine, iki tip hücre içermektedir. Modellerden biri yerel komşuluklu tek katmanlı, biri iki katmanlı diğeri de dünya küçüktür fenomeniyle kurulmuş iki katmanlı topolojiye sahiptir. Ayrıca sensör sıcaklığının farklı sınıflayıcı ve öznitelikler için sınıflama başarısına olan etkisi de tartışılmıştır.

1. INTRODUCTION

1.1 Purpose of the Thesis

Like audition and vision, olfaction provides most animals information about their surroundings. This information is gathered from odors which is a sensation caused by odorants around.

Many objectives may be introduced in order to solidify the necessity of odor classification by electronic terms, but the main motivation behind this need is the fact that both human and animals use the knowledge of odor from feeding and sexual behavior to identifying objects that are potentially dangerous such as fire, gas and poisonous food.

Odor information is widely used for various purposes. For example, for discrimination of two objects with similar appearances like water and alcohol, smelling is safer than tasting. Also for determining the quality of an object, usually food, smelling is preferred to tasting. Since olfaction system of dogs is very advanced, dogs are used for target tracking and search of non-metal objects like heroin and living organisms. Smelling is also a part of medical in diagnosis of certain respiratory and digestive system illnesses such as diabetes.

In order to provide olfactory information and process odors artificially, machine olfaction gave rise to developments in biological modeling, sensor technology and bio-inspired technologies. A bio-inspired application on olfaction is electronic nose.

In the past decade, electronic nose instrumentation has generated much interest worldwide for its potential to solve a wide variety of problems in fragrance and cosmetics production, food and beverages manufacturing, chemical engineering environmental monitoring, and more recently, medical diagnostics and bioprocess [2]. An electronic nose is a machine that is offered to detect the odorants around and process them to classify or give a decision.

Sensing is realized by various methods and advances in sensing depends on the developments of sensor technology. Sensor technology and instrumentation for electronic noses are commercially available but usually in desktop form, not suitable for mobile uses because of size, sensing abilities or power consumption. Since sensing part is a built-in system, pattern analysis and signal processing techniques can be applied by advanced processors, so algorithmic cost of these methods is not an issue in odor processing. However, odor sensory data is relatively new in signal processing era and olfactory processing deviates from auditory and visual signal processing because of nature of the signal. The principle difference results from the sensory level, sensors are short-lived, produced with high mismatch or are too slow to set on a stable response. Therefore, odor processing also aims to overcome these problems caused by odor sensors.

In this thesis, data collected with commercially available metal oxide gas sensors of Figaro Inc. are used. Then the sensory data is processed with the proposed Cellular Neural Network based artificial antennal lobes on transient regime in order to accelerate the decision interval, decrease the time required for classification. Not only the processing unit but also some sensory characters may have a positive effect on decision time so sensor temperature is also altered and its impact on classification performance is discussed.

In this thesis, Cellular Neural Network based artificial antennal lobe models are presented and an artificial olfaction system bench is offered to test these models. Advance that is brought by artificial antennal lobe model to the system is examined with different classification problems.

Chapter 2 gives a brief view on olfaction and summarizes biological background of olfaction system. Odor sensing and processing technologies are given in Chapter 3 together with the commercial electronic noses. Models for antennal lobe are introduced in Chapter 4 and they are tested in Chapter 5. Chapter 6 discusses effects of sensor temperature on classification performance. Finally, Chapter 7 concludes the efficiency of artificial antennal lobe on classification of odors.

2. OLFACTION

In this section, a brief introduction to olfaction concept in nature will be given and olfaction system on mammals and insects will be studied in detail in order to create an insight towards a bioinspired artificial odor processor.

2.1 Definition of Odor

An odor is the perception that arises when an odorant which is a compound generates a stimuli in the receptory part of olfaction system of an animal [2].

Like vision and audition, olfaction is vital for analyzing the surroundings odor signals of food, environment or other organisms carries concise information about feeding, sexual behavior and potential danger which are vital.

Odorants are usually organic compounds which are volatile and hydrophobic as well as some inorganic compounds such as ammonia and hydrogen sulfide.

It is important to note that, although the concentration of the odorant is very low in the air (in the orders of parts-per-billion or even parts-per-trillion) it can still be detected [4]. Therefore, not the concentration of the odorant but the molecular shape of it makes the odor recognizable. A trained human olfaction system is capable of distinguishing more than 10.000 odors [5]. However, not all the objects has an odor, but some compounds which have a molecular weight less than 300 dalton and which provide certain properties such as water solubility, sufficient water pressure, low polarity some ability to dissolve in fat (lipophilicity) and surface activity evokes sensory process [5].

Discovery of olfactory receptor (OR) genes by Buck and Axel [6] accelerated the researches on both physiological and biochemical behavior of the olfaction system and a great advance has been accomplished which leads the researches towards an artificial olfaction system. Odors can be labeled with the sensations that they raise for human, such as sweet or acidic [7].

2.2 Biological Olfaction

In vertabrates or in insects, stimuli to odorants are created on a similar path which starts at the olfactory receptors (ORs). Odorants are caught by ORs which are located on the olfactory epihelium in the nasal cavity in vertebrates or by the antenna in insects. A preprocessing unit called antennal lobe (for insects) or olfactory bulb (for human) follows the sensory part and leads the stimuli to the higher levels of nervous system for any type of decision such as classification.

2.2.1 Olfaction System of Insects

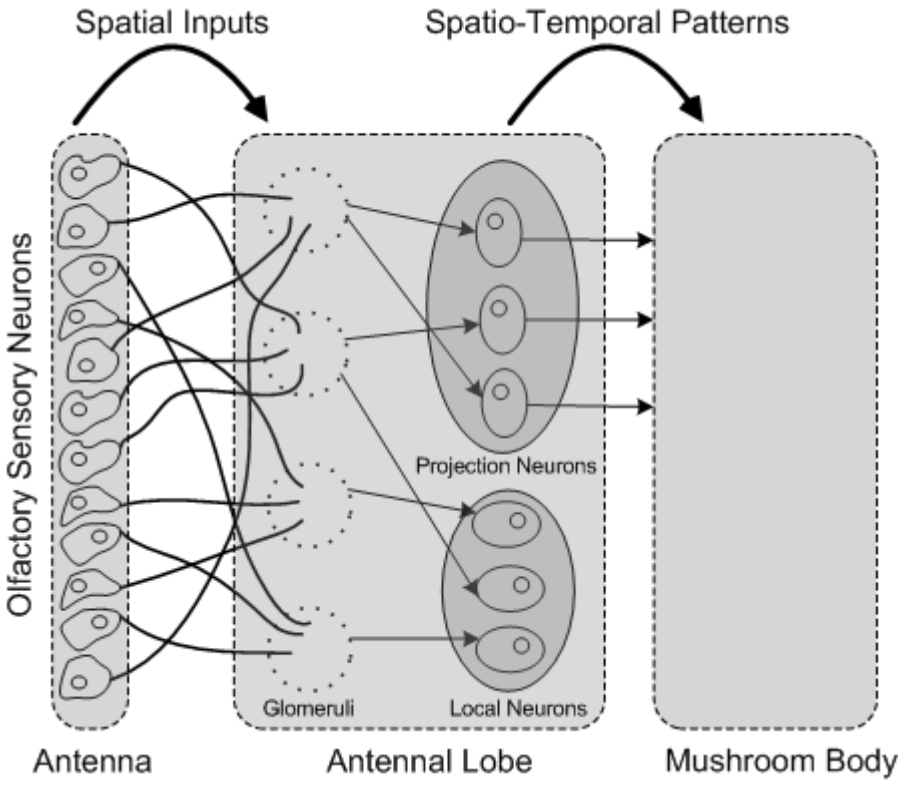

Figure 2.1 : A block-diagram interpretation of the generic insect olfactory system.

Having fewer neurons and receptors, insects are better models to imitate olfactory systems than more complex mammals. Studies on Drosophila give much information about olfactory system in insects. Olfactory system in insects is composed of three stages as shown in Figure 2.1. A sensory encoding of the stimuli by a vast diversity of receptors is captured by the projection neurons and local neurons which generate a spatio-temporal pattern. This pattern is read-out by the Mushroom Body in the form of static images (i.e., snapshots). This final layer is considered to be the generic classifier of the insect brain.

The first stage of olfaction is the antenna where odor information is gathered by the olfactory receptors. Although olfactory neurons which express the same kind of odor may include more than one neuron, they are all connected to the same glomeruli [8]. Glomeruli provide connection between olfactory sensory neurons and local neurons which are primarily inhibitory and projection neurons [9].

Odor discrimination is processed in higher layers of olfaction system where information is projected from antennal lobe by projection neurons. Therefore, effect of odorants on antenna neurons (primary neurons) is somehow moved to higher order neurons for discrimination [3]. One of the key points of olfaction in insects is how the receptors are connected to classification units called mushroom bodies. This projection is done in the antennal lobe, second stage of olfactory system.

Antenna: Olfaction is not the only function of antenna but the first stage of olfaction in insects is antenna where the ORs that detect the odorants are located. ORs are located in the chemosensory sensilla, which are not only present in insect antenna in palps and tarsa, but other organs of an insect. Odorants are taken into chemosensory sensilla via the cuticle pores and evoke the sensory neurons by collising with insect odorant binding proteins (OBPs) or Chemosensory proteins (CSPs) [10].

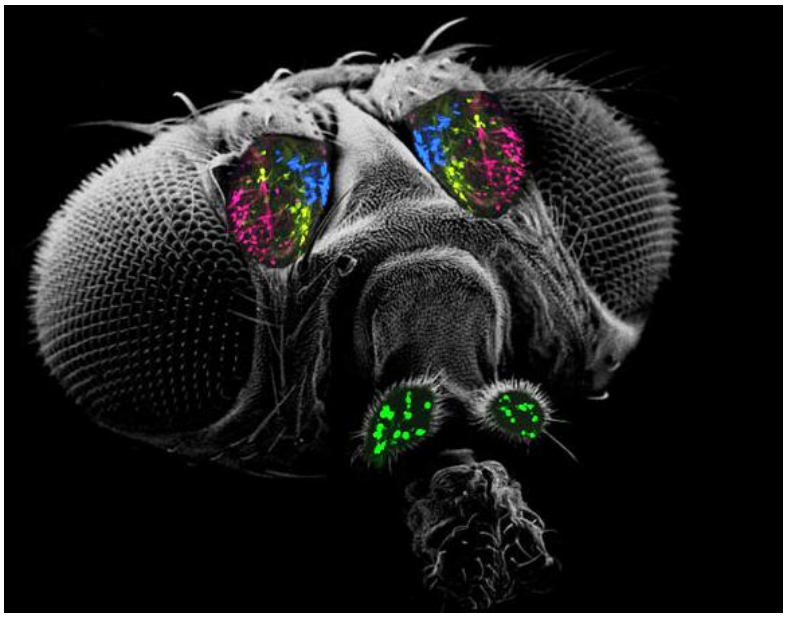

Figure 2.2 : Olfaction System of *Drosophilia* [1].

Olfaction system of *Drosophila* is partially shown in Figure 2.2. Green dots indicate the sensory neurons and two types of neurons together with glomeruli are highlighted with red, yellow and blue in the antennal lobe**.**

Antennal Lobe: Antennal lobe is the deutocerebral neuropil of the insect, which receives the input from the olfactory sensory neurons on the antenna. Functionally, it shares some similarities with the olfactory bulb in vertebrates.

The antennal lobe is composed of densely packed neuropils, termed glomeruli, where the sensory neurons synapse with the two other kinds of neurons, the projection neurons and the local neurons. There are 43 glomeruli in the Drosophila antennal lobe. The projection neurons project to higher brain centers such as the mushroom body and lateral horn of the protocerebrum. The local neurons, which are primarily inhibitory, have their neurites restricted to the antennal lobe. In Drosophila, each olfactory sensory neuron generally expresses a single olfactory receptor gene, and the neurons expressing a given gene all transmit information to one or two spatially invariant glomeruli in the antennal lobe. Moreover, each projection neuron generally receives information from a single glomerulus. The interaction between the olfactory receptor neurons, local neurons and projection neurons reformats the information input from the sensory neurons into a spatio temporal code before it is sent to higher brain centers. The plasticity and coding properties of the projection neurons are currently under intensive investigation at several laboratories.

Mushroom Body: The mushroom bodies or corpora pedunculata are a pair of structures in the brain of insects and other arthropods. They are usually described as neuropils, i.e. as dense networks of neurons and glia. They get their name from their roughly hemispherical calyx, a protuberance that is joining to the rest of the brain by a central nerve tract or peduncle. They were first identified in 1850 by the French biologist Félix Dujardin [11].

Mushroom bodies are known to be involved in learning and memory, particularly for smell. In larger insects, studies suggest that mushroom bodies have other learning and memory functions, like associative memory, sensory filtering, motor control, and place memory. They have been compared to the cerebral cortex of mammals. Because they are small compared to the brain structures of vertebrates, and yet many arthropods are capable of quite complex learning, it is hoped that investigations of the mushroom bodies will allow a clear view of the neurophysiology of animal cognition [11]. The most recent research is also beginning to reveal the genetic control of processes within the mushroom bodies.

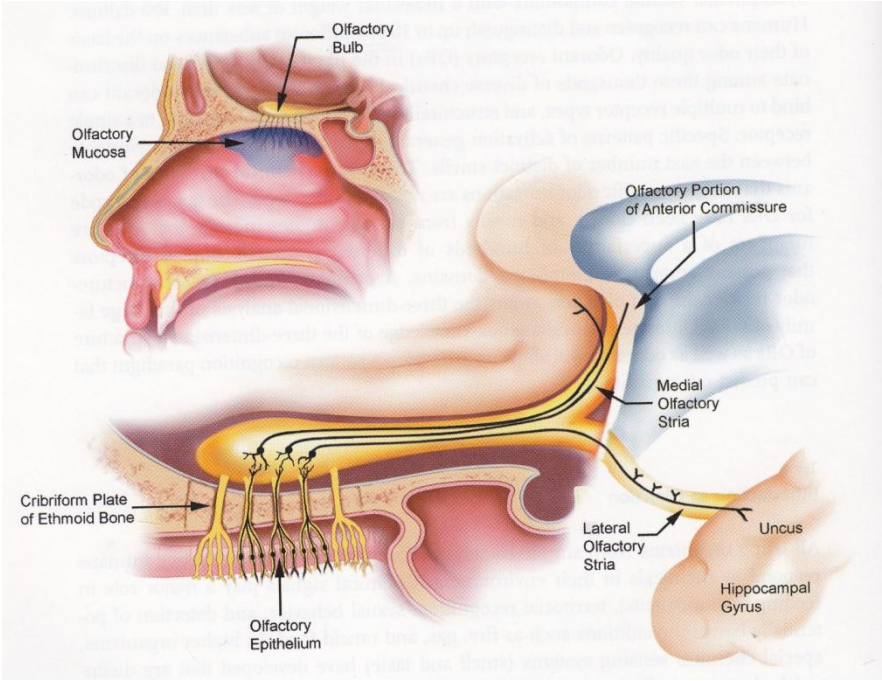

Figure 2.3 : Cross-section of the skull [2].

Most of our current knowledge of the mushroom bodies comes from studies of a few species of insect, especially the cockroach Periplaneta americana, the honey bee Apis mellifera, the locust and the fruit fly *Drosophila melanogaster*. Studies of fruit fly mushroom bodies have been particularly important for understanding the genetic basis of their functioning, since the genetics of this species are known in exceptional detail.

In the insect brain, the peduncles of the mushroom bodies extend through the midbrain. They are mainly composed of the long, densely packed nerve fibres of the Kenyon cells, the intrinsic neurons of the mushroom bodies. These cells have been found in the mushroom bodies of all species that have been investigated, though their number varies; for example fruit flies have around 2,500 whereas cockroaches have about 200,000.

2.2.2 Olfaction System of Mammals

Olfactory system of many mammals contains two distinct subsytems: main olfactory system, which detects volatile stimuli of odorants in the air, and an accessory olfactory system, which detects fluid-phase stimuli and especially evolved for sexual behavior. In this subsection, the main olfactory system will be investigated.

Olfaction system works in harmony with trigeminal receptors on tongue to enjoy the flovor because human tongue can distinguish only among a few types of taste where nose can distinguish among more [12]. However, this secondary function of olfaction system will not be covered here.

In air breathing animals, nose is covered by two types of epithelium partially, olfactory epithelium where the ORs are located and the respiratory epithelium. The ratio between them gives an insight about the olfactive sensitivity of the animal. In order to compare the olfactive sensitivity, some dogs have 170cm2 epithelium with more densely located receptors and they can distinguish up to 10000 different odorants [12].

In humans, the olfactory epithelium covers a surface of about 3 cm2 and is composed of three main cellular types: the olfactory sensory neurons (also called olfactory receptors), the sustentacular or supporting cells, and the basal epithelial or stem cells [13].

Sensing unit of air breathing mammals is placed in the nasal concha in nasal cavity. Odorants dissolved or cached by the mucus lining in nose and detected by ORs on the dendrites of the olfactory sensory neurons (OSNs). Detection is a process of binding the odorant to odorant binding proteins [6].

Molecules of odorants passing through the superior nasal concha of the nasal passages dissolve in the mucus lining the superior portion of the cavity and are detected by olfactory receptors on the dendrites of the olfactory sensory neurons. This may occur by diffusion or by the binding of the odorant to odorant binding proteins. The mucus overlying the epithelium contains mucopolysaccharides, salts, enzymes, and antibodies (these are highly important, as the olfactory neurons provide a direct passage for infection to pass to the brain).

The binding of the ligand (odor molecule or odorant) to the receptor leads to an action potential in the receptor neuron, via a second messenger pathway, depending on the organism.

Averaged activity of the receptor neurons can be measured in several ways. In vertebrates responses to an odor can be measured by an electroolfactogram or through calcium imaging of receptor neuron terminals in the olfactory bulb. In insects, one can perform electroantenogram or also calcium imaging within the olfactory bulb [13].

The receptor neurons in the nose are particularly interesting because they are the only direct recipient of stimuli in all of the senses which are nerves. Senses like hearing, tasting, and, to some extent, touch use cilia or other indirect pressure to stimulate nerves, and sight uses the chemical rhodopsin to stimulate the brain [11].

3. ODOR SENSING AND PROCESSING

Odor identification is a matter of labeling a coded sensor array data with the respective odor identity. Therefore two challenges arise, collecting the physical data that form an odor from environment which is sensing and properly coding the data for a successful decision is processing. In 1982 Persaud and Dodd [14] first brought up the idea of a device that uses chemical sensors for sensing the odors and uses pattern recognition. Very first researches on artificial olfaction are dominated in Warwick University Olfaction Research Group which also employs Persaud and Dodd, in 1987 group came up with the realization of the first electronic nose (e-nose) by the help of metal oxide gas sensors which are commercialized by Figaro electronics since 1968 [15]. From the first attempt to build artificial olfaction system, e-noses have showed plenty of advances with the innovations in sensor technology, signal processing and artificial intelligence. Discovery of odor binding proteins in 1991 [6] completed the missing theoretical gap in artificial olfaction systems and gave a rise to research on e-nose.

Since 90's, e-noses are being widely used in not only commercial industries such as food, cosmetics, security, agricultural and pharmacy but also research fields like biomedical, neurophysiology and chemistry and even medical diagnosis. The commercial use of e-noses provided support on artificial olfaction systems. Many electronic noses are commercially available today and have a wide range of applications in various markets and industries ranging from food processing, industrial manufacturing, quality control, environmental protection, security, safety and military applications to various pharmaceutical, medical, microbiological and diagnostic applications [16].

In this chapter, dominating odor sensing methods will be introduced and difficulties occur in the sensory level will be discussed then an introduction to odor processing will be given.

3.1 Electronic Nose

An electronic nose (e-nose) is an electronic device that is inspired from biological olfaction system and senses the odor in the environment with an array of odor sensors and processes the data gathered from the sensor array for classification, control or decision. Olfaction is a determination method that we widely use daily. For example, when we examine if a food gone bad, we use olfaction or the odors of certain chemicals notifies danger. However, human nose can go saturation under continuous flow of the same odor, therefore a human nose cannot be used as a process controller in a food production line or as a gas detector.

An electronic nose has typically two main parts: a sensor array and a processing unit. Structure of sensor array is determined by the aroma sensor technology and the processing unit is designed according to the application and usually is an artificial neural network, software with digital pattern-recognition algorithms or reference-library databases [16].

3.2 Sensors Used in E-Noses

Odor identification is a difficult and, compared to the visual or the auditory domain, a unique pattern recognition task. As defined in the previous chapter, odorants are molecules therefore physical state of them cannot be discussed, but odorants are pretended to be seen as gases because in human olfaction starts at nose which is also an organ in respiration system. Therefore, smelling always thought with breathing although there is a secondary olfaction system in the most mammals that can smell the liquids. Even though vertebrate secondary olfaction system can smell liquids, electronic devices that contain liquid sensors are classified as electronic tongues and ones that contain gas sensors are named as electronic noses [17], but the types of gas sensors that are used in electronic noses vary: two major groups are mass sensitive chemosensors and metal oxide gas sensors.

The basic principle of electrochemical gas sensors is to convert the interactions between gaseous molecules and sensor-coating molecules to electrical current detectable by a transducer that converts the modulation into a recordable electronic signal [18]. Sensor coating materials (semiconducting metal oxides, photo diodes, organic/inorganic film layers etc.) and detection principle (mass sensitivity, resistance change, current or voltage change etc.) changes type to type.

3.2.1 Challenges in Odor Sensing

Gas Sensors used in an e-nose sensor array should achieve some specs according to the needs of the system and environment that e-nose is designed for. For example, sensitivity of a sensor should be high enough to perform like biological nose but high sensitivity also effects selectivity of the sensor that, higher the sensitivity sharper the selectivity. A specific sensor should have high sensitivity to that type of odor and less to others in order to increase the selectivity. E-noses are not only used for discrimination but also quality control applications to detect one type of odor definitely.

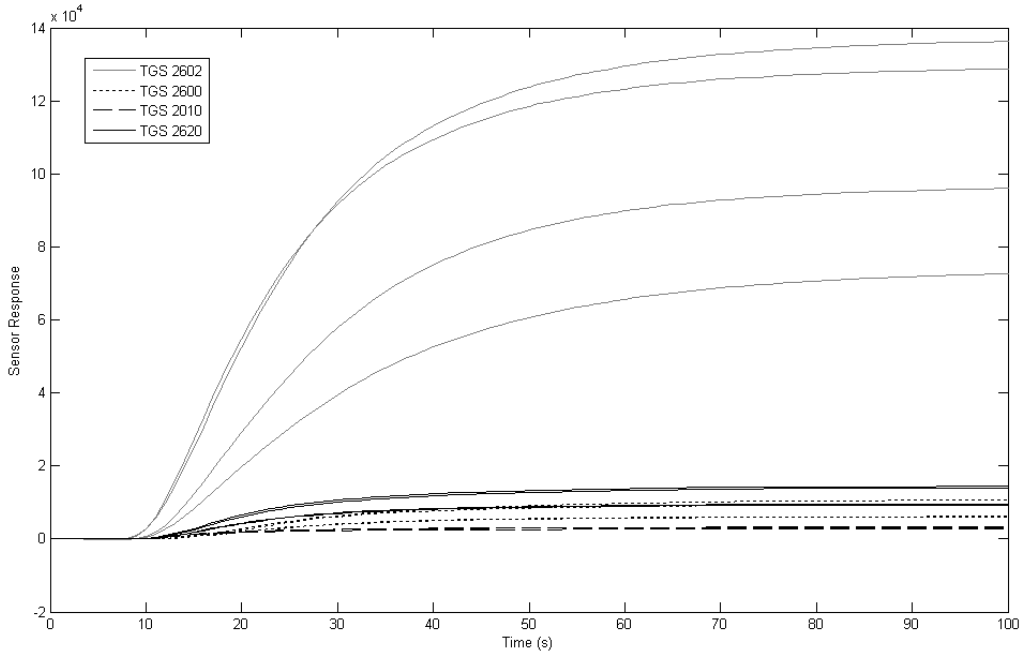

Figure 3.1 : Response of a sensor array of Figaro Metal oxide gas sensors to Acetaldehyde under constant flow and temperature.

Environment of an e-nose can be an uncontrolled open-air field if so, sensor array should be more robust to noise and variable change such as temperature and humidity. Moreover power consumption is another issue for mobile e-nose systems such as odor tracking robots and discrete odor detectors for home security systems. If the system is working on a volatile bench, power consumed can be paid as a prise for accuracy or speed. However as the other sensing systems, sensor technology is going smaller and more suitable for portable environments.

Considered with the challenges in processing, the main handicaps in odor sensors are related to speed of the sensors. The time required for a sensor to settle on a stable activation level is preferred to be short but as it is seen in Figure 3.1, typical settling time is around 100 seconds for metal oxide gas sensors. Another criterion that determines the speed of the sensor is the recovery time. The time needed to return back to neutral level under dry air after being exposed by a certain odor is called recovery time.

Moreover, sensors should be calibrated and characteristic of them should be investigated since sensors of the same family may react different to same type of odors due to the mismatch. This also effects the training phase of the processing part. Sensors may get exhausted during the measurements so they need to be cleaned and the characteristic of it may also change during the measurement or from one measurement to another.

As nature of odors, they change in time quickly so any change in target odor can be considered as noise or vice versa. Odors are not like visual or audio signals; they do not stay in the same concentration at one point and cannot be cached easily. Even for the vacuum systems, noise is an important problem. In order to overcome this problem, sensor level improvements are not enough; it should be supported by improved processing techniques.

3.2.2 Metal Oxide Gas Sensor

Metal oxide gas sensors was introduced in market in 1968 in Japan to be used as household gas alarms in Japan [15]. Then the industrial usage is widened with other kinds of sensors. A semiconducting metal oxide layer is used as the sensing material. Sensing material is placed on a ceramic sheath and an internal heater. The principle is based on the resistivity change of the metal oxide crystal which is usually SnO_2 doped with small amounts of metal additives. Doped sensors show greater sensitivity to oxygenated volatile organic compounds (e.g. alcohols, ketones, etc) than to aliphatic, aromatic or chlorinated compounds [19]. Doping with Pt and Pd increases the sensitivity of SnO_2 sensors to gases such as benzene and toluene [19]. When the sensitive layer is heated at a certain temperature by the internal heater adjusted by the technician, oxygen is absorbed on the crystal surface with a negative charge and the conductivity of the surface decreases. Resistance of sensor is determined by the potential barrier formed by absorbed oxygen in the boundaries. In the presence of volatile molecules, absorbed molecules and metal film layer interact in terms of absorption or depletion of oxygen. In the presence of a deoxidizing gas, carriers are pulled above the surface so sensor resistance is decreased as shown in Figure 3.2. In summary, sensing is based on an oxygen exchange between the volatile gas molecules and the metal coating material [16]. Electrons are attracted to the loaded oxygen and result in decreases in sensor conductivity [20].

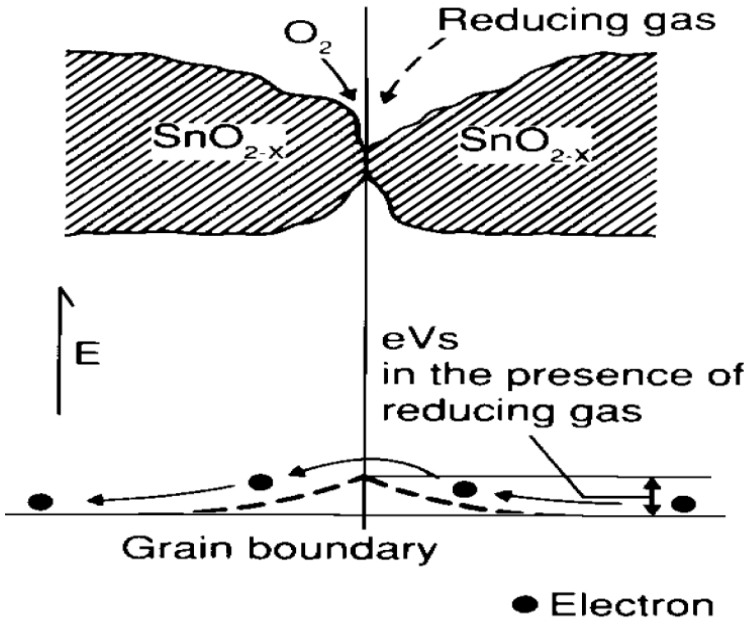

Figure 3.2 : Model of Taguchi MOS Gas Sensor [3].

Change in resistivity of the sensor is cohesive to the type of gas molecule, concentration and any other effects on absorption - depletion mechanism such as humidity and layer temperature together with the partial pressure of oxygen.

Relationship of a sensor resistance to gas concentration is linear on a logarithmic scale within a practical range of gas concentration [3]. Due to the logarithmic dependence of the sensor response on the concentration of volatiles, loss of sensitivity arises (towards low-volatile aroma compounds) in the presence of highly concentrated detectable species such as ethanol [21].

The sensitivity and selectivity of MOS sensors are determined by the choice of the semiconductor material. Modifications are induced by doping the semiconductor with noble metal catalysts (e.g. Pt, Pd, Al, Au), by modulating the operational temperature (e.g. 200°C - 500 °C) or by introducing thermal gradients/cycles [22]. Metal oxide sensors have relatively high sensitivity even around sub-ppm (parts per million) level for some gases, but this sensitivity comes with and expense of poor precision, for a good precision Quartz crystal microbalance (QCM) sensors can be used but they are not suitable for mobile or commercial use since they have a complex circuitry. On the other hand metal oxide sensors do need only a small circuit just to monitor or convert the conductivity change on the surface for the desired environment such as a processor. Although they have response time order of tens in seconds, M-metal oxide sensors are still faster than most of the other sensor types both in response and recovery time.

While the sensor is working under high internal temperature, power consumption of the heater is another drawback. Some other sensors such as electrochemical sensors have lower power consumption in expense of sensitivity.

3.3 Odor Processing

There are plenty of producers who manufacture e-noses and most of them produce processing units together with sensors. Gardner and Bartlett who introduced the concept of e-nose for the first time state the necessary components of an e-nose [18] as:

- a transfer system for odor molecules from the source to sensor array,

- sensor array chamber that provides suitable temperature, humidity, flow and pressure for the array,
- a circuitry that converts chemical signal into electrical signal,
- an analog to digital converter,
- processor suitable for the purpose.

First three bullets should be organized according to the sensor type chosen. Gardner and Bartless clearly states that the components, advances in sensor and materials technology favors the decision on sensory level but the processing unit and algorithms require totally different expertize.

Two types of analysis on odors are used in the prior works: transient analysis and steady state analysis which is more common.

Steady state analysis means waiting for seconds and generating features from the stable activation level a sensor reach. For a classification problem it is necessary to use features not changing in time therefore it is not a surprise that this analysis type is very popular. Commercially available e-noses analyze raw steady-state sensor response in three ways [23]:

- Graphical analyses: bar chart, profile, polar and offset polar plots.
- Multivariate analyses: principal components analysis (PCA), canonical discriminant analysis (CDA), feature weighting (FW) and cluster analysis (CA).
- Network analyses: artificial neural network (ANN) and radial basis function (RBF).

Among the others, graphical analysis is the simplest data reduction technique and it is suitable for searching an unknown analyte in a reference database. This can be a powerful analysis if the samples are distinct enough to be compared visually.

For electronic-nose data analysis, multivariate analyses are very useful when sensors have partial-coverage sensitivities to individual compounds present in the sample mixture [16]. Supervised and unsupervised methods are valid in this group where all of them are linear. Unsupervised methods such as PCA and CA, are preferred when a library of target odors is not available and provides a strong discrimination between samples recorded and displays the hidden relationships between analytes. On the other hand, several prior measurements should be recorded in order to be statistically consistent then characteristics of new measurements can be compared with the characteristics of known samples.

Network analyses such as ANN and RBF methods are very powerful and are inspired by the way the mammalian brain processes information [24]. Supervised classifications are common with ANN and RBF and as a difference from others they have nonlinear characteristic. The nonlinear character of this method makes it interesting specially for non-linear technologies such as MOS [25]. Nonlinearity of processing also increases the noise tolerance of the e-nose. Work of Srivastava [26] shows that, neural network processing of transformed data gathered from SnO_2 type metal oxide sensor array has better noise tolerance.

As stated above drift of a sensor can be blocked or life time of a e-nose can be extended by effectively changing the sensor type used in the array but the problem of response time remains more or less the same for all type of sensors. Therefore to overcome this problem considering the dynamics of the sensor system and analyzing the transient response is required. The speed of sensor response is a handicap not only for artificial systems but also for biological beings. Under constant gas concentration, it takes hundreds of milliseconds an olfactory sensory neuron to settle on a stable activation level [27]. The fact that discrimination of odors is finished earlier [28], gives an insight that antennal lobe plays a crucial role by spatio temporal coding on classification of transient data. There are many works [29] that processes the transient response of the sensor array and states the importance of transient as a matter of both speed and biological relevance.

In the case of using raw transient response, the total number of features for each odor sample is equal to the product of the number of sensors in the array and the number of odor samplings (each “sniff”) per measurement [34]. As a result, a known problem in machine learning called *the curse of high dimensionality* [41] arises and it results in overfitting in the design of the odor classifier [34].

In order to survive from dimensionality problem, order of sensor array can be reduced by choosing the sensors which have different sensitivity and selectivity profiles and less correlation with others for the ongoing odor application. Another way is to generate feature rather than the raw transient response. These methods include the ones that employ uncommon properties of sensors such as [36] and the ones preprocessing the raw data in order to generate a new feature that carries the information coming in time such as [40].

4. ARTIFICIAL OLFACTION SYSTEM MODELS

This chapter is the report of an artificial olfaction system model which is proposed to overcome the speed problem mentioned in the previous chapter, and respecting the biological researches done on *Drosophila* and vertebrates. Vital issue in odor processing is time and to fasten the classification process, a preprocessing unit is developed that is inspired from biological structures antennal lobe and olfactive bulb.

4.1 Overview of An Artificial Olfaction System

Roughly, olfaction system is composed of three major parts which perform three duties:

- Sensing: Reacting to odorants around either with electrochemical signals
- Feature Extraction: Changing spatial sensor response into spatio temporal patterns
- Processing: Evaluation of produced patterns: classification and decision.

Smelling begins at odor sensory neurons with perception of volatile odorants and producing electrochemical response. Like there exist different kind of sensory neurons responding diversely to different environments, there are several metal oxide sensors types classified according to doped metal. Either in antenna or nose, odor sensory neurons employing same kind of odor binding protein meet in the same glomeruli. As it is shown in Figure 4.1, perception layer of an artificial nose is sensor array and it is matched with odor sensory neurons together with glomeruli. The upper layer is named as feature extraction although a complete model for this section is not introduced yet, its function on odor processing is to project suitable features to higher nervous sytem levels. The most important benefit of this layer is to fasten the decision by going beyond the limits of sensory neurons. Generation of spatio-temporal patterns from spatial sensor response is actualized in this thesis.

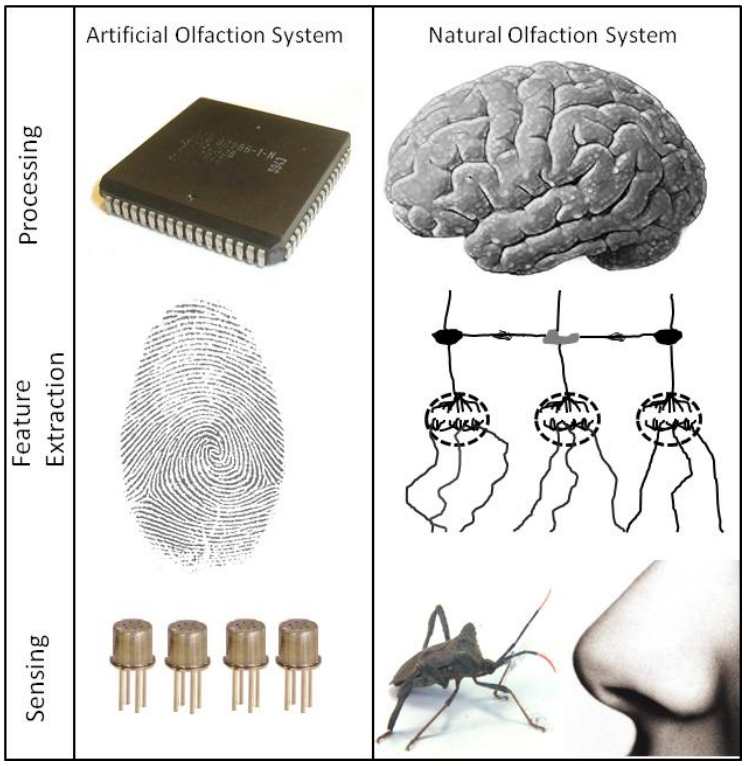

Figure 4.1 : Analogy between an artificial olfaction system and a natural one.

The processing unit shown in olfaction diagram can either be part of olfaction system like olfactory cortex or any other part in brain. Therefore, that part does not benefit on olfaction system directly but uses the olfactory information. In this thesis, processing unit is assumed to be a classifier in order to test the models (Chapter 5).

4.2 Neuron Population Model

It is probably true that studies of primitive nervous systems should be focused on individual nerve cells and their precise, genetically determined interactions with other cells. Although such an approach may also be appropriate for many parts of the mammalian nervous system, it is not necessarily suited to an investigation of those parts which are associated with higher functions, such as sensory information processing [43]. Therefore, for odor sensor processing response of the neuron population is more important than activation of individual neurons in the antennal lobe or olfactive bulb. The models given below are build up investigating the research on *Drosoplia* so they will be called as artificial antennal lobe models.

There are two types of populations in the antennal lobe, one excitatory and one inhibitory. These populations are adapted to Wilson-Cowan population model as introduced in [31], and given as:

$$\beta_i^E \frac{dx_i(t)}{dt} = K_i^E \Theta(-\sum w_{ij}^{EI} y_j(t) + g_{inp}^E S_i^E) - x_i(t) + \mu_i^E(t) \qquad \textbf{(4.1)}$$

$$i = 1,2,...N_E$$

$$\beta_i^I \frac{dy_i(t)}{dt} = K_i^I \Theta(\sum w_{ij}^{IE} y_j(t) + g_{inp}^I S_i^I) - y_i(t) + \mu_i^I(t) \qquad \textbf{(4.2)}$$

$$i = 1,2,...N_I .$$

In Equations (4.1) and (4.2), superscripts E and I are used for excitatory and inhibitory populations and x_i and y_i stand for the projection neurons (excitatory neurons) and local neurons (inhibitory neurons).

Every excitatory neuron has one external input, S_i^E and several inputs from inhibitory neurons which it is connected to and weighted by w_{ij}^{EI}. An excitatory neuron is connected to inhibitory neuron, y_i, with a probability of ½. g_{inp}^E is a fixed conductivity, same for all neurons in the excitatory population and Θ denotes unit ramp function.

The gains K_i^E and time scales β_i^E vary for every neuron in the reference model and drawn from exponential distribution. μ_i^E is the additive white noise process.

Inhibitory population has the same structure and same constants with excitatory population.

As in biological structure, same type of neurons are not connected to each other. External input (sensor response) of a projection neuron is excited by the neuron, but in order to prevent this excitation go infinity, the sensor response is decremented by inhibitory neurons connected to that projection neuron. The collaboration of inhibition and excitation is the key procedure of odor sensory processing.

4.3 Cellular Neural Network (CNN) Based Artificial Olfaction Models

Cellular Neural Network (CNN) [44] is an information processing system composed of a large number of simple analog signal processing elements, called cell, which are locally interconnected and which cooperate to perform parallel processing in order to solve a given computational task. The key concept distinguishes a CNN from the other neural networks is that the interconnections among the cells are local.

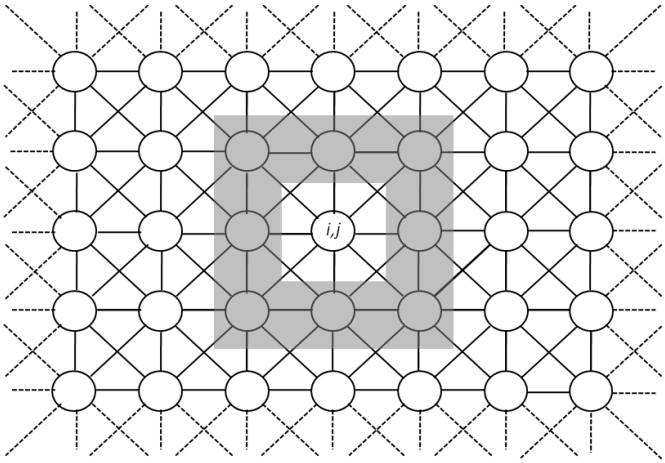

Figure 4.2 : A 2-D CNN with radius 1.

Formal definition of CNN is given in [45]:

Cellular Neural/Nonlinear Network (CNN) is any spatial arrangement of locally-coupled cells, where each cell is a dynamical system which has an input, an output and a state evolving according to some prescribed dynamical laws.

A 2-D CNN, as shown in Figure 4.2, has *NxM* cells denoted by *C* and each is locally coupled only to those neighboring cells which lie inside the region $\mathbf{S_{i,j}(r)}$ with radius **r**,

$$S_{i,j}(r) = (C_{k,l} : \max(|k-i|, |l-j| \le r, 1 \le k \le N, 1 \le l \le M, k \ne i, l \ne j)) \qquad \textbf{(4.3)}$$

One of the pioneering work in CNNs study, is "The CNN Universal Machine: An Analogic Array Computer [46]", where the first algorithmically programmable, analog CNN processor was introduced to the engineering research community. In order to avoid input/output connection with the external world on CNN-UM, Roska and Chua [46] proposed the integration of an array of sensors on the same semiconductor substrate.

Today, mixed-signal integration of CNNs enables to direct interface to sensory device such as ACE16k [47], which is specially designed for image processing applications. Fusing the sensory and the processing circuitry on the same chip is helped to overcome the drawbacks of real time signal processing of traditional digital computer. Hence, CNN based processors are an alternative computer for real-time signal processing.

4.3.1 One Layer CNN

Regularity of a CNN is in contrast with randomness of the antennal lobe model. Moreover, a regular CNN contains same type of processors, the firsth attempt to develop an artificial antennal lobe from a CNN is to introduce two types of populations which expose similar dynamics with each other and given in Equation (4.1) and (4.2).

First of all a 2-D CNN of NxM is created on a regular grid with an ordinary connection template A and same type of processors shown in Figure 4.3(a). In Figure 4.3 (a), each cell is connected to its neighbors lie inside radius 1. Then randomly chosen half of them are labeled as excitatory neurons and the others inhibitory ones. The connections between inhibitory-inhibitory and excitatory-excitatory neurons are broken as shown with dashed lines in Figure 4.3(b). In Figure 4.3(b), black nodes represents inhibitory neurons and white nodes stand for excitatory ones. Therefore the connection matrix A is no more valid.

Mathematical model of neurons is inspired from the reference model and a new model is developed in [42]. If neuron is labeled as an excitatory neuron, $x_{i,j}$, model of that neuron is given by

$$\beta \frac{dx_i(t)}{dt} = K.\Theta\left(-\sum_{l=-r}^{r}\sum_{k=-r}^{r} A_{k,l}.C_{i+k,J+l}(t) + g_{inp}S_{i,j} \right) - x_{i,j}(t) + \mu_{i,j}(t) \qquad \textbf{(4.4)}$$

$$i \in 1,2,...n, \qquad j \in 1,2,...m, \qquad C_{i+k,j+l} \in C_{in}$$

where $C_{m,n}$ stands for inhibitory neurons, if there exist an inhibitory neuron with index *n,m* and **r** gives the radius.

For other neurons, which are inhibitory, only the excitatory neurons in the influence area are taken into consideration by equation

$$\beta \frac{dy_i(t)}{dt} = K.\Theta\left(-\sum_{l=-r}^{r}\sum_{k=-r}^{r} A_{k,l}.C_{i+k,J+l}(t) + g_{inp}S_{i,j} \right) - y_{i,j}(t) + \mu_{i,j}(t) \qquad \textbf{(4.5)}$$

$$i \in 1,2,...n, \qquad j \in 1,2,...m, \qquad C_{i+k,j+l} \in C_{in}.$$

The template A is given as

$$A = \begin{bmatrix} A_{-1-1} & A_{-10} & A_{-11} \\ A_{0-1} & A_{00} & A_{00} \\ A_{1-1} & A_{10} & A_{11} \end{bmatrix}.$$

A neuron has at most eight connections if all the neurons in its neighborhood is from the opposite population. However, it may also have no connection if it is from the same type with its neighbors.

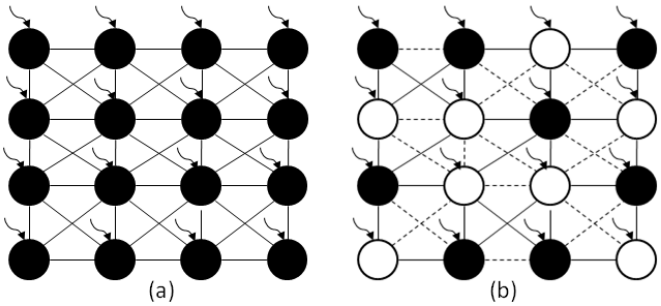

Figure 4.3 : 2-D CNN with (a) same type of processors, (b) two types of processors.

Note that, setting a connection to -1 is not in harmony with the biological background inspired. From the equations (4.1) and (4.2), it can be clearly seen that, an excitatory neuron is fired if the input to that neuron from a sensor is greater than the sum of inputs from the inhibitory neurons, in other words, odor information arriving a projection neuron should compensate and exceed the effect of local neurons connected to that projection neuron.

On the other hand in CNN based model, if an inhibitory neuron is southern or northern neighbor of an excitatory neuron, input of that inhibitory neuron would excite like sensory input. Similarly, an excitatory neuron would work like an inhibitory neuron if it is southern of northern neighbor of a neuron. Therefore, we cannot talk about global excitatory or inhibitory neurons, but every neuron may behave as excitatory or inhibitory according to their neighbors.

4.3.2 Two Layer CNN

A CNN grid composed of two types of processors is not likely to be realized because it does not match with the idea of regularity. Also with a network such that, a template is not valid any more.

Then, another attempt to introduce different cell dynamics on the same system is done by proposing the following two layer CNN. For two layer CNN, a layer of size N/2xM is built on a regular grid and duplicated with different cells. Consequently, one layer of inhibitory cells and one layer of excitatory cells are created, mathematical models of each cell are identical in the layer. As connection inside the population is not allowed, connection template for inhibitor layer and excitatory layer is given by a zero matrix.

As shown in Figure 4.4, each cell from inhibitor layer is connected to the cells in excitatory layer with the template

$$\hat{A} = \begin{bmatrix} \hat{A}_{-1-1} & \hat{A}_{-10} & \hat{A}_{-11} \\ \hat{A}_{0-1} & \hat{A}_{00} & \hat{A}_{00} \\ \hat{A}_{1-1} & \hat{A}_{10} & \hat{A}_{11} \end{bmatrix}.$$

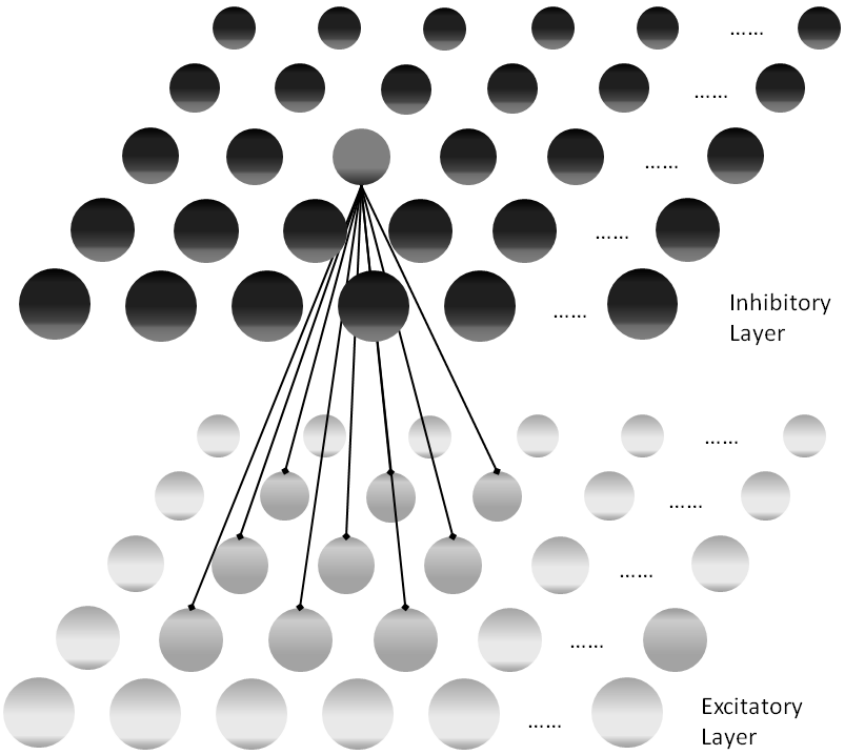

Figure 4.4 : Two layer CNN

One layer consist of inhibitory neurons and second layer contains only excitatory neurons, so that all the neurons in the same CNN layer has the same mathematical model. In Figure 4.4, connections of an inhibitory neuron in upper layer to neurons in the excitatory neuron are given with template Â. Mathematical model of excitatory and inhibitory layer neurons are given by

$$\beta \frac{dx_{i,j}(t)}{dt} = K.\Theta\left(-\sum_{l=-r}^{r}\sum_{k=-r}^{r} \hat{A}_{k,l}.y_{i+k,J+l}(t) + g_{inp}S_{i,j} \right) - x_{i,j}(t) + \mu_{i,j}(t) \qquad \textbf{(4.6)}$$

and

$$\beta \frac{dy_{i,j}(t)}{dt} = K.\Theta\left(\sum_{l=-r}^{r}\sum_{k=-r}^{r} \hat{A}_{k,l}.x_{i+k,J+l}(t) + g_{inp}S_{i,j} \right) - y_{i,j}(t) + \mu_{i,j}(t) \qquad \textbf{(4.7)}$$

respectively.

In this topology, every neuron except for the ones on the edges has exactly nine connections. Therefore, one neuron has more connections than 1-layer CNN topology which is presented in Section 4.3.1.

4.3.3 Small World CNN

Small world phenomena was introduced in 60's and redescribed for networks by Watts and Strogatz [48]. Since then small-world phenomena is widely used in networks from neural networks to social networks.

Small world phenomena is adapted for discrete time Hopfield networks [49] and in 2001 Bohland et al. [50] suggested that, small world networks are more efficient in terms of resource utilization then randomly connected sparse networks and some other research on associated memory - retrieve a memorized pattern, supported that idea.

Neuron connections in biological neural networks are not only deterministic but they own randomness [51]. Researches on nervous system of *C. Elegans* showed that, its biological neural network is constructed with a small-world like topology [52].

Not only the connections of a neuron affect the efficiency of the neural network, some research are presented about the importance of breaking the symmetry and varying connection weights.

Small world phonemona suggests to develop *short cuts* [48] between neurons which do not have direct connections. Therefore *charasteristic path length (CPL)*, average length of the shortest path between pairs of neurons, is decreased.

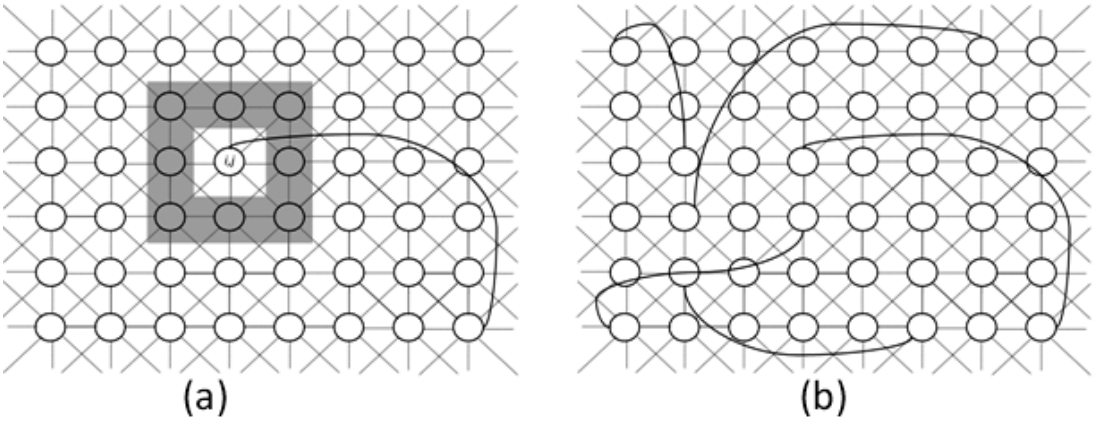

Figure 4.5 : Small World CNN (a) p=1/n and (b) 1/n<p<1.

It is claimed by Yang and Chua [53] that, while all the cells are connected to the ones, which are defined in its neighborhood, all the cells are in touch with each other directly or indirectly via other connections, so CNNs present the dynamics of a small world neural network. However, in 2003, the term Small world CNN is introduced [54] and a few researches on performance of this network on image processing are presented.

In Figure 4.5(a), all neurons have their own local couplings and one randomly chosen neuron have one additional connection with a random neuron which is not in its neighborhood, $\mathbf{S_{i,j}}$. Probability of random connection is the ratio number of neurons chosen for additional connections to number of neurons and given by *p*.

5. TESTS FOR PROPOSED MODELS

Previously proposed models will be tested in this section. Key point of the models is that, they are designed to convert spatial sensor response into spatio-temporal patterns as an antennal lobe do in insect olfaction system. The goal of the antennal lobe models includes two branches, one is to achieve better performance in classification of odors according to the chosen problem. The other one is to reach a satisfactory high performance earlier in the transient.

The purpose of the tests is to check the validation of the models with its biological background. Note that the propose is not to build a complete artificial olfaction system, but in order to display the act of artificial antennal lobe models clearly, complete artificial olfaction system is drawn for some of the tests below. In order to examine the performance dependent on process unit shown in Figure 4.1. Support Vector Machine (SVM) [55] is used as a classifier with two different training algorithms.

However, efficiency of the artificial antennal lobe should be reported independent from the classification tool so success of it in increasing and accelerating the separability of sensor data is tested. Principle component analysis (PCA) and mutual information (MI) are the two such methods and widely used for sensory data classification problems.

Input data are drawn from real measurements done in BioCircuits Institute, University of California San Diego. In this section, an overview of measurement set up is given and results of performance test with and without classification tool are reported.

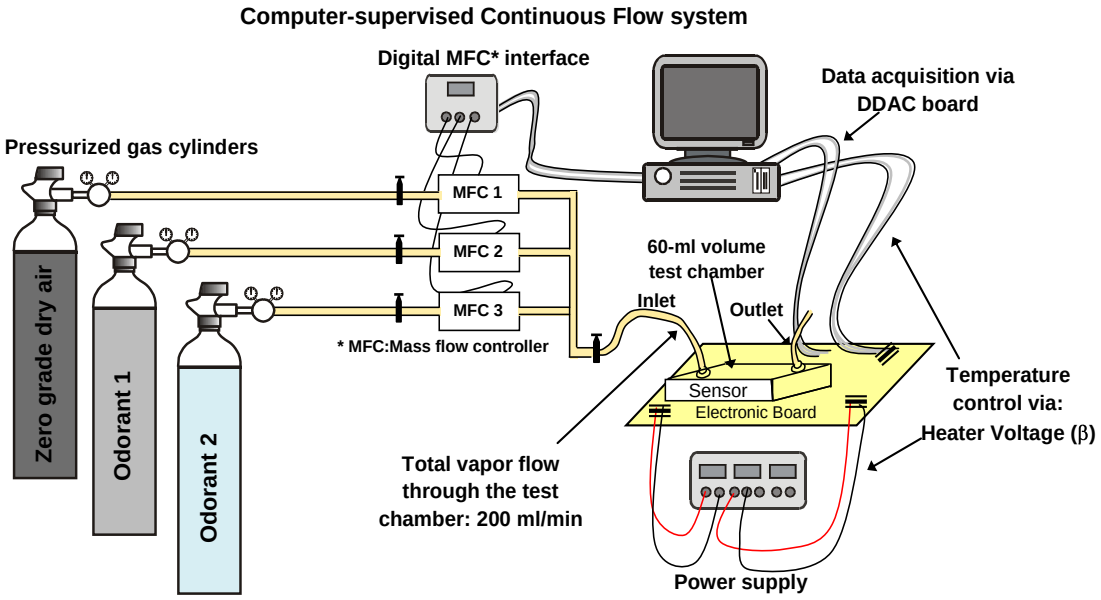

Figure 5.1 : Measurement Setup.

5.1 Measurement Setup

Measurement setup is given in Figure 5.1 (A. Vergara, BCI, UCSD). All the system is computer-supervised by Labview. The odorants with desired concentration is streamed into the sensor chamber where 16 metal oxide gas sensors of Figaro Inc., namely TGS2600, TGS2602, TGS2610 and TGS2620 [3] are placed. Heater voltage of the sensors are controlled by Labview in order to adjust the internal temperature of the sensors. The odorants (gases) and dry air are stored in pressurized gas cylinders and the amount of them streaming to the sensor chamber is controlled by mass flow controllers (MFC) via digital MFC interface. Mass flow control is used to compose a mixture of desired ratios or adjust the concentration of target odor. The flow of vapor through the chamber is kept constant by MFC. The sensor activation is converted into a resistive signal by a simple electrical circuit on electronic board and signal is collected from the board.

5.2 Problem Definition

With the measurement setup given in the previous section, two problem sets are gathered. The first one, Set A, involves three classes: pure acetaldehyde, pure toluene and mixture of those two. Concentration of the gas is adjusted by the dry air so a vapor of desired concentration is carried. Vapor from one class is steamed into the test chamber under constant temperature (40^o C) for 100 seconds and the sensor data is collected with a sampling frequency of 100 Hz after injection. After injection the chamber is cleaned with dry air flow. 20 measurements are recorded for both pure acetaldehyde and pure toluene, 10 times for each of acetaldehyde-toluene mixtures which have the following compositions: 96\%-4\%, 98\%-2\%, 2\%-98\%, 4\%-96\%.

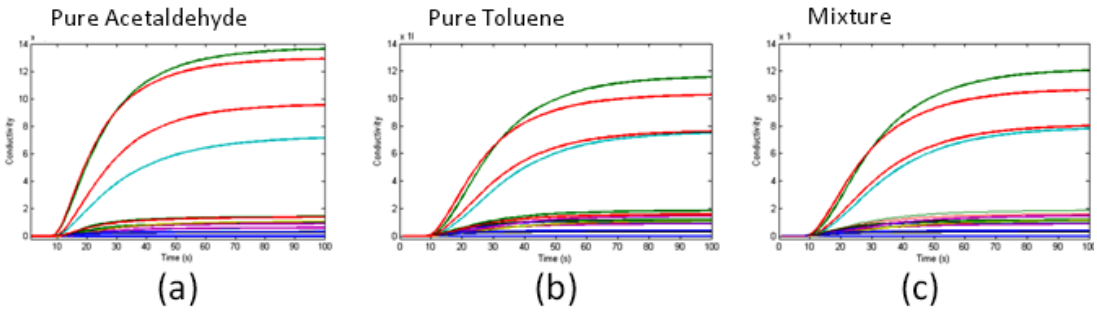

Figure 5.2 : Sensor response for Set A.

Examples of measurements, one of each class, is shown in Figure 5.2. The data set is 80 repeated records which offset is removed from each. Therefore a data set of three classes, two pure odors and mixtures of them as a third class, is created.

Set B, which contains five types of odor is used to test SWCNN. A sensor array containing 16 metal oxide sensors (same measurement setup in Set A) is used to collect information of the following odors: acetaldehyde, acetone, butane, ethylene and ethane. The sensors in the gas chamber are exposed to those gases one by one under constant flow and temperature for 100 seconds after the chamber is cleaned with dry air. Fifteen measurements for each odor is recorded.

Another data set, Set C is created for another three class problem but is rather simple because three different odors are used. In this data set, number of sensors in the array is decreased and the performance of sensor array is aimed to be increased by changing the sensor temperature. Effect of sensor temperature on performance is investigated in the next Section 6.

5.3 Tests for CNN Based Models

Highly correlated variables do not increase the distinguishability of a data set while they carry more redundant information than uncorrelated variables. It is possible to foresee the separability of a data set by looking at statistical information such as correlation between the variables.

CNN based models are tested using Set A and with three classification tools, namely principle component analysis (PCA) and support vector machines (SVM). Each measurement of data set A is expanded with white noise with a variance of 0.5 and applied to CNN based models: the models are driven by random noise for 50 seconds and the measurement is applied at time zero. After 100 seconds, the system is continued to be driven by noise for 50 more seconds.

Data set A is applied to 1 layer CNN and 2 layer CNN described in Section \4 and the results of excitatory processors are collected as antennal lobe model output because as given in Section 2, only the activity of projection neurons are transferred to the higher layer and projection neurons are represented as excitatory cells in the models.

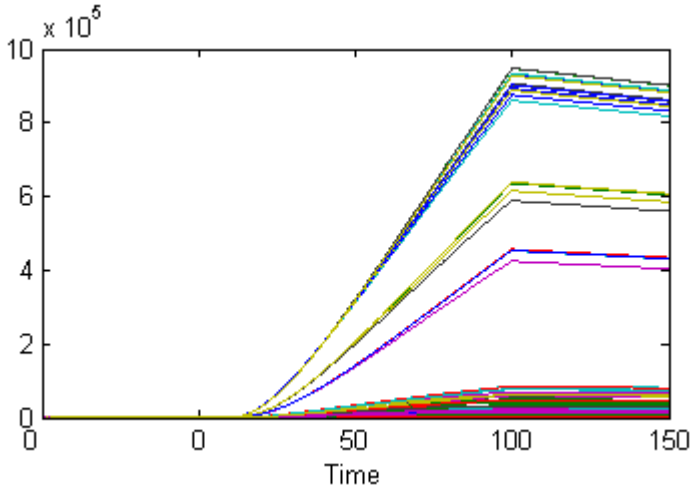

Figure 5.3 : Output of 1 layer CNN for pure acetaldehyde.

For 1 layer CNN, a network of 10x15 is created with the connections explained in the previous section and half of the cells are labeled as excitatory and other half is inhibitory. Therefore 75 of the cells are excitatory and their output is recorded. In Figure 5.3 output of 75 excitatory neurons for pure acetaldehyde is given. The measurement is exposed from time 0 to 100. In the test procedure the response to sensory input is used, not the output for the noise and that is the period between 0 and 100 seconds in Figure 5.3.

In order to discuss the performance of CNN based models in terms of connections, another model named *uncoupled model* is used for comparison. This uncoupled model involves 75 excitatory and 75 inhibitory cells, which perform the same dynamics with the proposed CNN cells. However, there is no connection between cells so the dynamics ends up with the form

$$\beta_i^E \frac{dx_i(t)}{dt} = K_i^E \Theta(-g_{inp}^E S_i^E) - x_i(t) + \mu_i^E(t) \qquad i = 1,2,...N_E \qquad \textbf{(5.1)}$$

$$\beta_i^I \frac{dy_i(t)}{dt} = K_i^I \Theta(-g_{inp}^I S_i^I) - y_i(t) + \mu_i^I(t) \qquad i = 1,2,...N_I\,. \qquad \textbf{(5.2)}$$

5.3.1 Principle Component Analysis

Principle component analysis (PCA) is a simple method for extracting appropriate information from complex and high order data sets such as sensor array responses. Therefore PCA is a widely used method for discriminating odors by sensor array process. Some recent research on odor classification based on PCA using MOS sensors are given in [56].

PCA was invented in 1901 by Karl Pearson [60]. This data analysis tool re-express the data set with most meaningful information by calculation of the eigenvalue decomposition of a data covariance matrix. The new data set is named with component scores and loadings and they have no dimension.

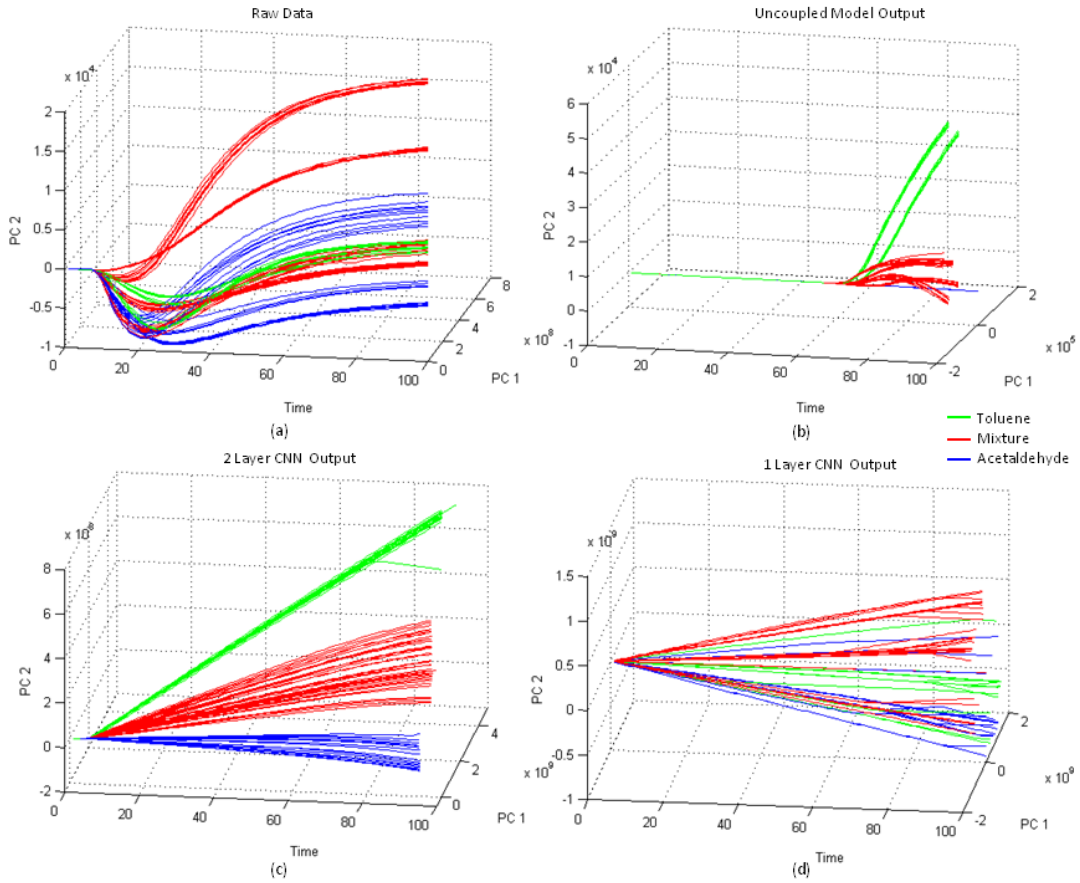

Figure 5.4 : Change of principle components in time (a) for raw data, (b) for uncoupled model, (c) for 2 layer CNN based artificial antennal lobe and (d) for 1 layer CNN based artificial antennal lobe.

Mathematical definition of PCA is given in [61] as an orthogonal linear transformation that transforms the data to a new coordinate system such that the greatest variance by any projection of the data comes to lie on the first coordinate (called the first principal component), the second greatest variance on the second coordinate, and so on.

First and second principle components for data set A is shown in Figure 5.4. The x-axis is the time axis because the change of principle components in time determines the increase in discrimination between classes in time.

As shown in Figure 5.5, principle components belonging raw data (sensor array output) for three classes do not show significant difference but both of the CNN based artificial antennal lobe model outputs are in the form that can be clustered in this early time in the transient and the in the case for uncoupled model, principle components of pure acetaldehite can be allocated from other two classes already.

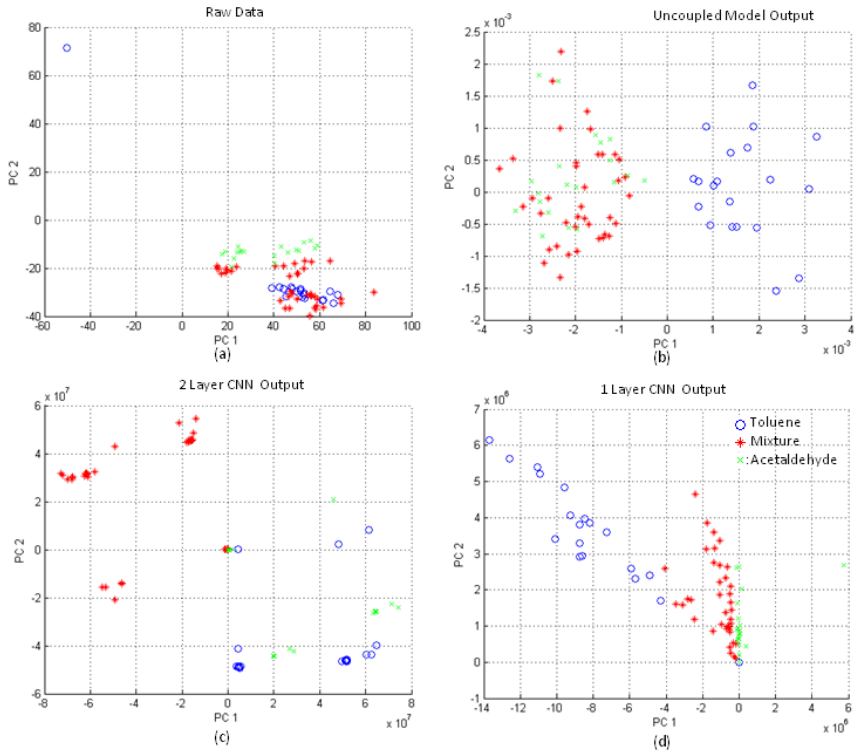

Figure 5.5 : Principle components at T=5s (a) for raw data, (b) for uncoupled model, (c) for 2 layer CNN based artificial antennal lobe and (d) for 1 layer CNN based artificial antennal lobe.

The principle components for T = 100, which means the steady state sensor response is given in Figure 5.6. Classes can be discriminated from each other by clusters for both of the four graphs.

In order to give detail about the change of principle components in time, Figure 5.7 is given. There, it can be clearly seen that, classes has become separable by T = 25 s for 2 layer CNN output.

5.3.2 Support Vector Machine

Support vector machine (SVM) pioneered by Cortes and Vapnik [62] is a supervised learning method used for classification or regression like multilayer perceptrons and radial-basis function networks. For this problem, it is used as a classification tool. Basically, support vectors assist to data points that are not linearly separable to be mapped in another space where they are separable. Therefore, an SVM model is a representation of mapping so that, data points from different classes can be divided by a clear wide gap.

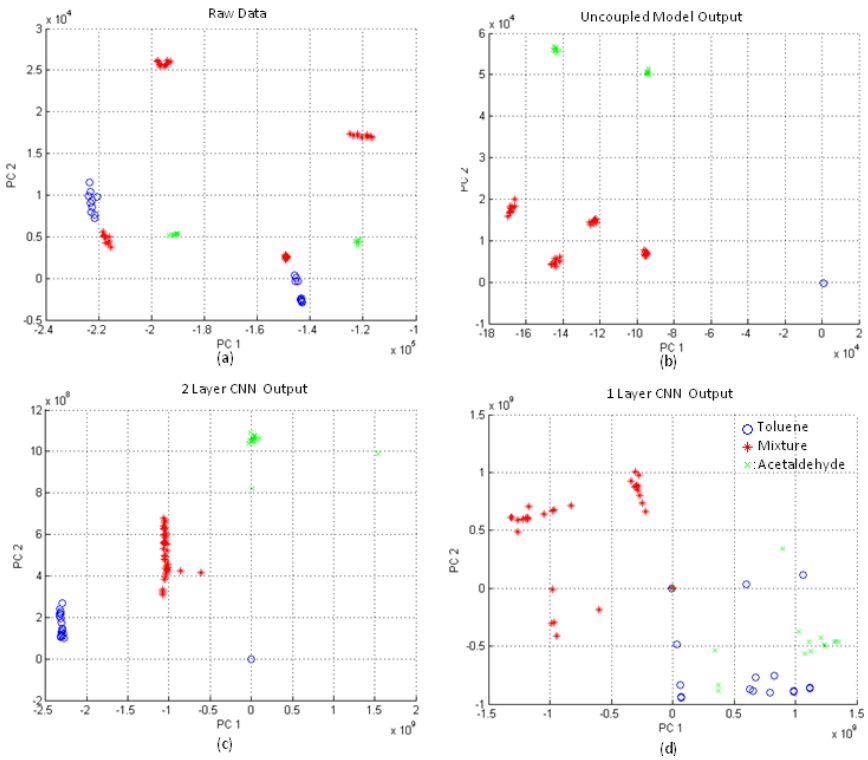

Figure 5.6 : Principle components at T=100s (a) for raw data, (b) for uncoupled model, (c) for 2 layer CNN based artificial antennal lobe and (d) for 1 layer CNN based artificial antennal lobe.

The main idea of a support vector machine is to construct a hyperplane as the decision surface in such a way that the margin of separation between positive and negative examples is maximized [63]. This aim is directed by method of structural risk minimization of statistical learning theory. This induction principle is based on the fact that the error rate of a learning machine on test data is bounded by the sum of the training-error rate and a term that depends on the *Vapnik-Chervonenkis dimension*; in the case of separable patterns, a support vector machine produces a value of zero for the first term and minimizes the second term [63].

In this thesis, a public available SVM tool, LibSVM [55] is used as classifier. As in the case for PCA, output of the excitatory processors are collected to be classified.

For each time T, projection neuron (excitatory processor) outputs are put together in a vector of length N_E and labeled with its class. For 80 records, 80 patterns that labeled with one of the three classes are obtained at every time snap. These labeled vectors are used as SVM inputs. SVM is trained with a linear kernel and leave one out technique is used for validation.

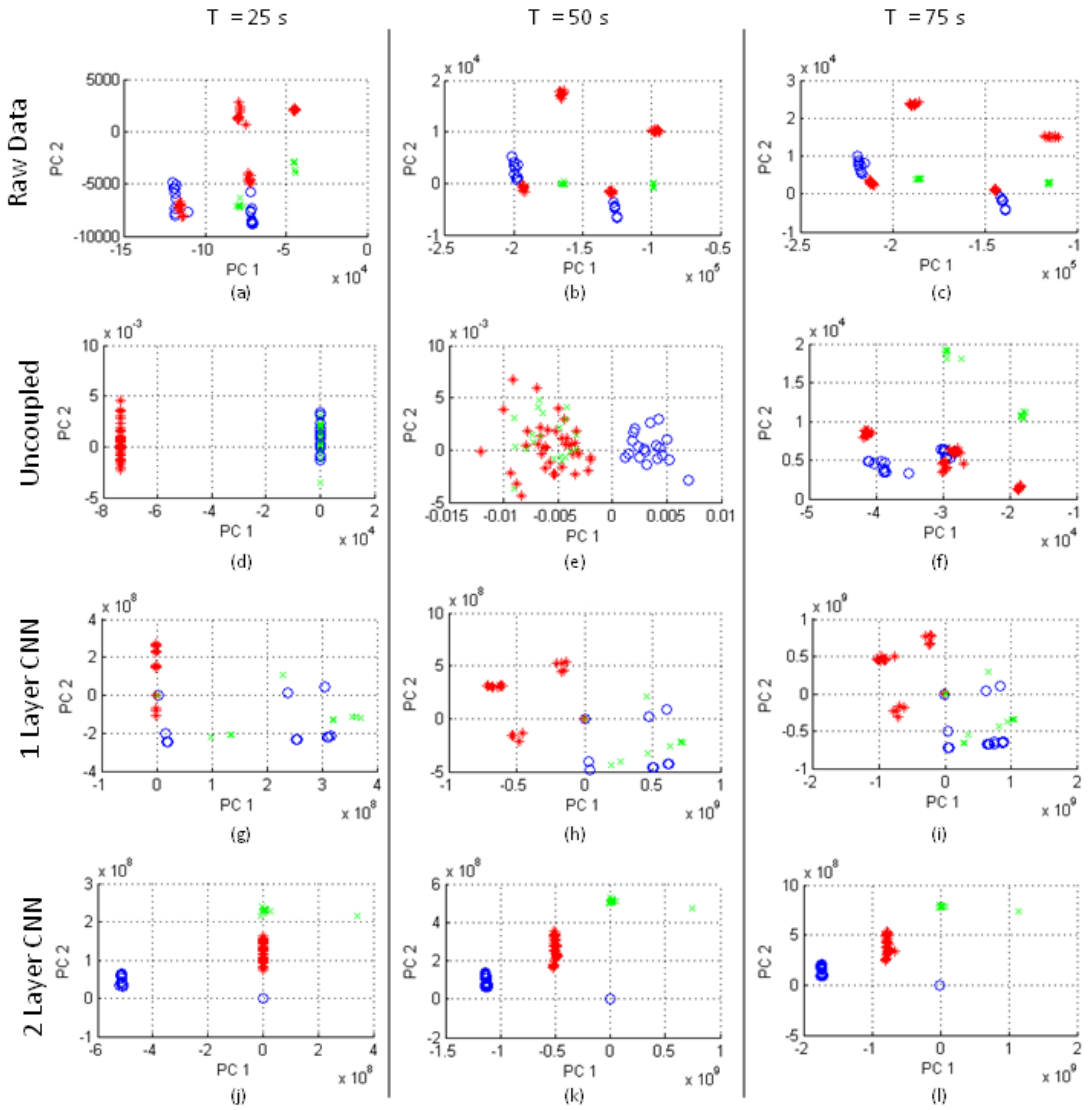

Figure 5.7 : Principle components for raw data, uncoupled model, 2 layer CNN and 1 layer CNN in the rows and at T=25s, T=50s, T=75s in the columns.

Two types of performance evaluations are done. One assuming system has memory and one considering every snapshot as a different classification problem.

*System without memory***:** Projection neurons in AL gives nearly constant output to MB [31]. Movement of information from AL to classification layer is repeated in single time samples. Instant activity of projection neurons can be considered as input of classification layer [31]. SVM module projects snapshots on excitatory neuron outputs. One pattern is randomly left out for test and SVM is trained with other 79 labeled patterns.

This procedure given in Figure 5.8 is repeated for 20 times with different test pattern. If the decision of SVM is same as the label of test pattern, that trial is counted as a success. Overall performance at that time snapshot is $100x\frac{\#success}{20}\%$ [42].

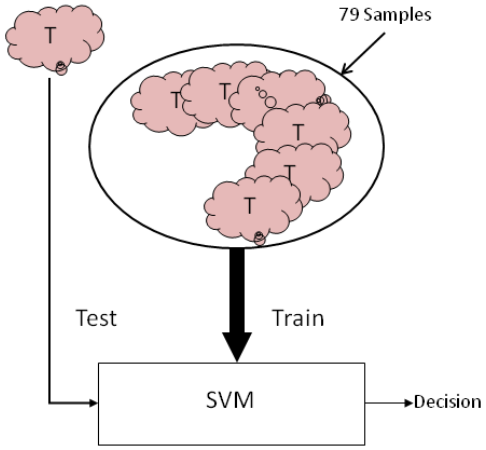

Figure 5.8 : Process for testing the system without memory.

The performance of CNN based models and uncoupled models are given in Figure 5.9. Estimated curves for test results when input is started to be read at T = 0 till T = 100. Curves are fitted with polynomials where RMSE of 1 layer CNN, 2 Layer CNN and uncoupled curves are 10.5481, 11.5857 and 10.4164 respectively.

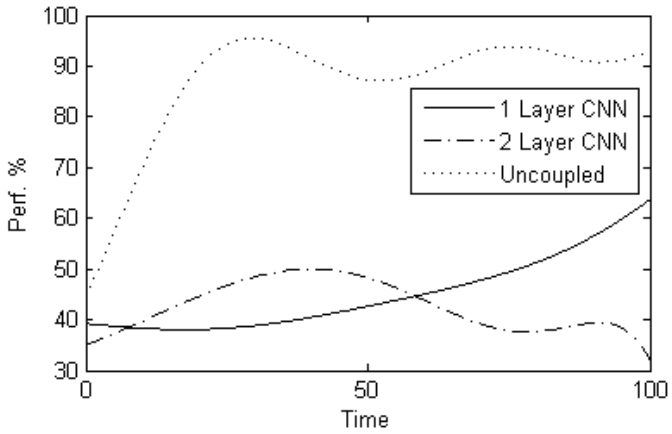

Figure 5.9 : Results for memoryless system.

It can be seen that, performance of classification increases in time but the PCA results were providing a better performance. Therefore it is obvious that the classification tool used is highly important in showing the real performance of the antennal lobe model.

As a comparison, the performance of 2 layer CNN increases faster than 1 layer CNN in small amounts up to a point. The number of connections can cause this.

However, for these models, parameter search and optimization is not done for this data set. Therefore, a classification tool test like this SVM test does not show the true performance of the models but may give an insight about the effect of dynamics since the performance of uncoupled model is satisfactory enough for some applications, even for this difficult classification problem. Change in parameters like gain, time constant, connection weights and connection matrix will definitely affect the performance.

*System with memory***:** As indicated above, the classification tool or training method can affect the performance so that they may be altered in order to find the best tool and method for this problem. Support vector machine is the second tool examined with this data set, so in this subsection the training phase of SVM is changed. In the memoryless case, all the time snapshots were considered as individual problems so distinct training sets and SVM models were build for each. However, in a real time application, no one can be sure about a pattern belongs to which snapshot exactly. Moreover, if the system is already on up to time T then there is no reason to dismiss the previous snapshots in decision. The system with memory is initiated with these motivations.

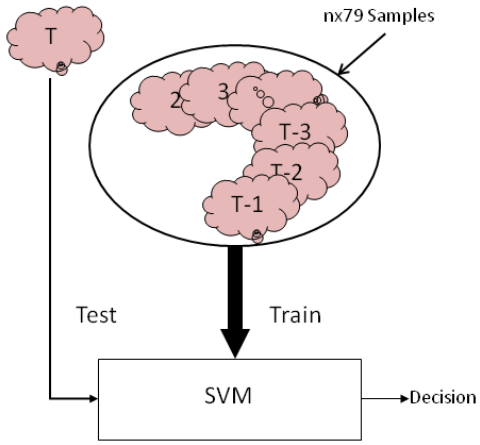

Figure 5.10 : Structure of the system with memory.

Introduced olfactory system with CNN based antennal lobe is depicted in Figure 5.10 for this case. As shown in Figure 5.10, from time 0 up to time T-1, all the patterns are saved as training set of SVM. Then, at time T, SVM is tested by patterns of snapshot T. Performance of the model is equal to the performance of SVM at time T.

Estimated curves for test results are shown in Figure 5.11, curves are fitted with polynomials where RMSE of 1 layer CNN, 2 Layer CNN, Raw Data and uncoupled curves are 10.8041, 11.2813, 12.2475 and 15.1173 respectively. CNN topologies give higher scores than uncoupled topology after the input is applied. Another point is that, with this training method a performance of nearly 80 % is achieved within the first 20s after the input is applied which is faster than the previous training case. The performance of the CNN model is higher than the raw data classification in the first seconds of the record. As a result, better performance can be achieved earlier by reducing the number of connections between neurons and using a regular structure instead of a random architecture if classification method is changed as indicated in this section [42].

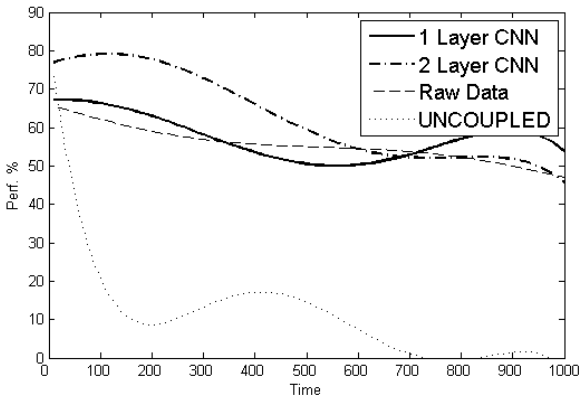

Figure 5.11 : Results for system with memory.

5.4 Tests for SWCNN Based Model

Small-world CNN based artificial antennal lobe model is tested with the data set B which contains five types of odors. Aim for the tests is to find out the effect of small-world phenomenon on odor classification problem rather than showing the performance of another CNN based artificial antennal lobe model with a different problem. The healing of using spatio-temporal patterns in stead of spatial sensor responses is already shown with the previous tests.

In this tests, gain in performance will be observed by increasing the number of neurons which make random connections.

The classification tool is selected as SVM and it is trained as a memoryless system, so every single snapshot is a different problem. However, leave one out technique is not used for validation. The SVM is trained with 60 of the patterns generated at time T and 15 patterns are used for test. Then the pattern set is shuffled and this procedure is repeated ten times. The performance in test set for each trial is recorded and the average performance of ten trials is accepted as the performance of the SWCNN at that time T.

A two layer SWCNN of size *4x4* is build with the template

$$A_1 = \begin{bmatrix} A_{-1-1} & A_{-10} & A_{-11} \\ A_{0-1} & A_{00} & A_{00} \\ A_{1-1} & A_{10} & A_{11} \end{bmatrix} = \begin{bmatrix} 1 & 1 & 1 \\ 1 & 0 & 1 \\ 1 & 1 & 1 \end{bmatrix}.$$

Except for the neurons at the edges, neurons have eight local couplings and total number of neurons in two layers is 32. The ratio of neurons that build a random connection to all neurons is given with p_c. All the neurons are allowed to build at most one random connection. Therefore, value of p_c changes between 0 to 1.

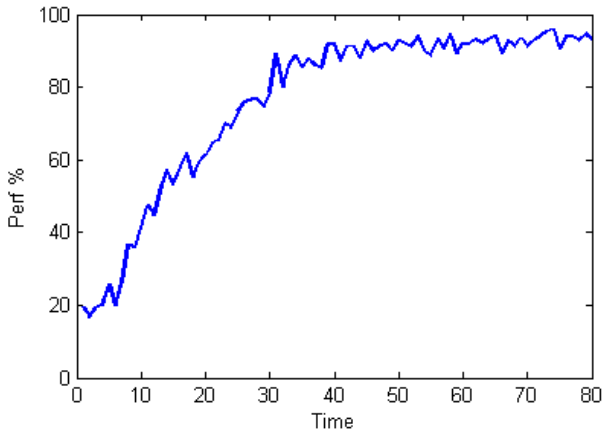

Figure 5.12 : Classification performance of SWCNN for template $A_1$and p_c=0.

In figure 5.12, increasing performance of the network designed as a basis for SWCNN can be monitored. The question is if the number of random connections can increase the performance. Each of the *p* cells randomly chosen from the excitatory layer made a short cut to an inhibitory neuron which it is not locally coupled. If all the neurons in the excitatory layer have one random connection, then *p* is equal to 16 and p_c =1. *p* also gives the number of random couplings.

Performance test is applied those 16 cases for five times: the edges of random connections are randomly changed, then the average performance is recorded. All those 16 cases are given in 5.13. Earliest time that the system achieves its maximum performance is not changed much.

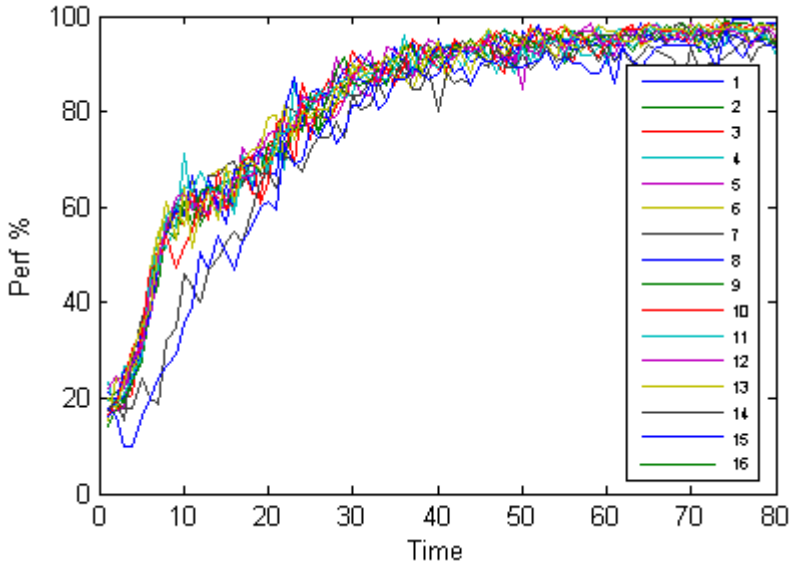

Figure 5.13 : Classification performance of SWCNN for template $A_1$and $1 \leq p \leq 16$.

The network is driven by 16 sensors in the cases above but can the increasing number of random connections compensate loss of sensor data in the sensor array? To answer this question, the cells in the network are driven by the same sensor. Firstly the performance of the network with only local couplings is given in Figure 5.14. When Figure 5.14 and Figure 5.12 are compared, the maximum classification performance is decreased when the sensor array data is lost.

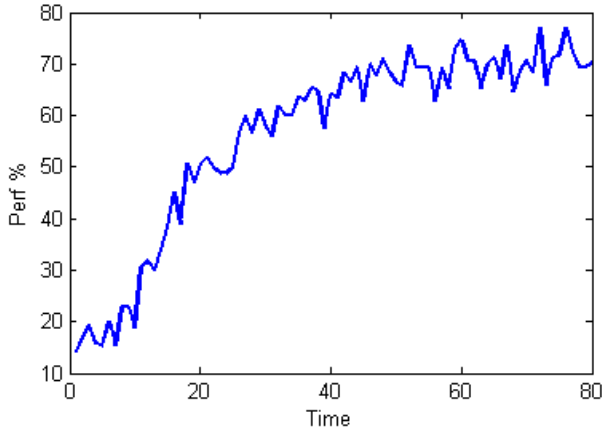

Figure 5.14 : Classifcation performance of SWCNN for template A_1 and $p_c = 0$ driven by one sensor

However, it is still slightly higher than the performance of raw sensor data given in Figure 5.15. Figure 5.15 regarding to classification performance of raw sensor response is not smooth; performance varies in time sharply because the number of measurements is not enough, so a fitted curve with an RMSE of 11.22 is given with a thicker line.

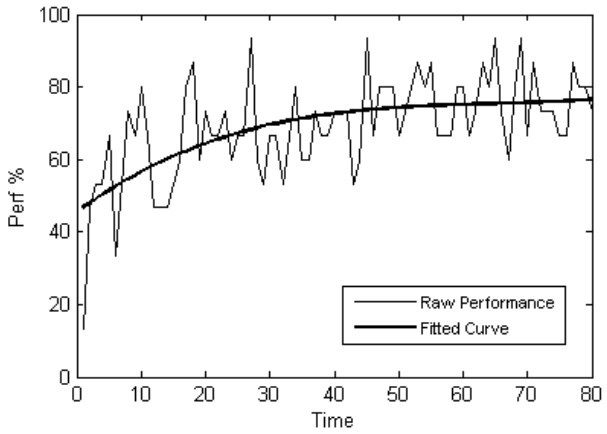

Figure 5.15 : Raw data classification.

Number of random connections are limited to 16 in those scenarios, a more clear observation is tried to be done by enlarging the network layers to a size of *8x8* and increasing the number of sensors to 16 again. The performance change is given in Figure 5.16 changing p from 1 to 64 in steps of four for clarity.

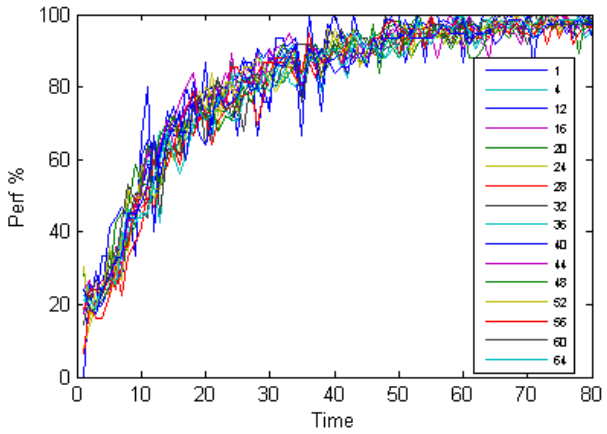

Figure 5.16 : Classifcation Performance of 128 cell SWCNN for template A1 and 0≤pc≤1

6. EFFECT OF SENSOR HEATER ON CLASSIFICATION PERFORMANCE

This chapter aims to give an further look to odor classification problem to improve the performance of classification success and rate by changing the parameters in sensory level. Inner temperature of the metal oxide gas sensor has a great impact on selectivity of the device, because the rate of reaction for each odor compound is releated with the absorption rate and amount of oxygen on the surface layer and this action is effected by surface temperature [64].

There exist two distinct phenomenons on influence of temperature modulation, one is stated by Morrison, as *temperature programming of the sensor is not a common technique used for selectivity* [13]. On the other hand, some recent research demonstrated that temperature modulation of metal oxide gas sensors can be used to increase the performance on classification [64] [66]. Temperature modulation obviously changes the response of the sensor to the same volatile odorant but it should be indicated when this change has a positive influence on selectivity of the sensor. Each data set, each classification problem shows a different character as each time snapshot is considered as a different classification problem. Lee et al. [64] states that temperature modulation or control can be used to improve the selectivity and sensitivity of semiconductor gas sensors, this is possible because each analyte gas has a characteristic conductance vs. temperature (or applied heater voltage) profile for each sensor type. Using the same commercial metal oxide gas sensors, information gathered from the sensors can still be increased by changing the voltage of sensor heater externally.

This chapter tries to find an optimum sensor temperature for a set of three-class problem empirically. A fixed optimal temperature is not valid at every snapshot in the transient. Moreover, best temperature varies due to the feature extracted from sensor data and the identification method used.

In this chapter, optimal temperature is tried to be obtained regardless of antennal lobe models. Three types of features are used for this purpose: raw data, integrated data and exponential moving average which is a popular smoothing technique in time-series analysis and described in Section 6.2.

The four identification methods namely mutual information, support vector machine, k-NN and naive Bayes classifier are given in Section 6.3. Then another test is given for two layer CNN based antennal lobe model in Section 6.4 using only one identification method: SVM.

6.1 Data Set

A data set containing three classes ammonium, acetaldehyde and acetone is formed by recording the response of sensor array in the gas chamber described in Section 5.1. The gas chamber is exposed by each of these gases under constant gas temperature for 100 second after the chamber is cleaned with dry air. The sensor array response is recorded and records rescaled to 100 seconds with 100 examples after the offset is removed. Thirty-nine trials are done for each of three classes.

This procedure is repeated for different sensor temperatures. Sensor temperature is adjusted by heater voltage. Heater voltage is increased from 4.5V to 5.5V with steps of 0.1V. The interval corresponds to nearly 300ºC-500ºC.

Therefore, eleven datasets belonging to different sensor temperatures are obtained and they are classified individually.

For the first part of examination, which does not cover CNN, based antennal lobe, two of the metal oxide gas sensors, TGS2600 and TGS2610, are used, two time series are labeled with the class name. Two more types of features are generated based on this two sensor data. The examples of those time series can be found in Figures 6.1, 6.2 and 6.3.

6.2 Feature Selection

Raw data (unprocessed sensor data) is used as feature. The two dimensional snapshot is taken at each second and labeled with the class of the odor so a set of 117 patterns are generated for 100 time slots.

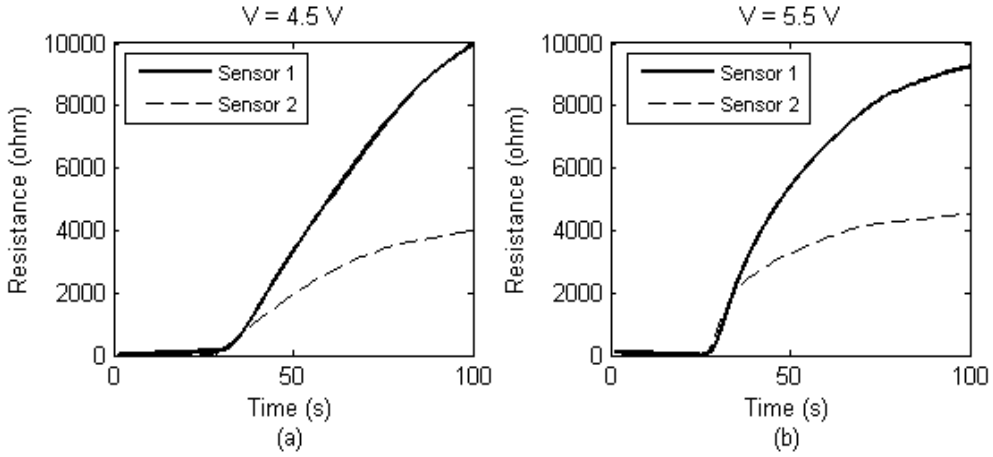

Figure 6.1 : Response of two sensors for ammonium when heater voltage is (a) 4.5V and (b) 5.5V

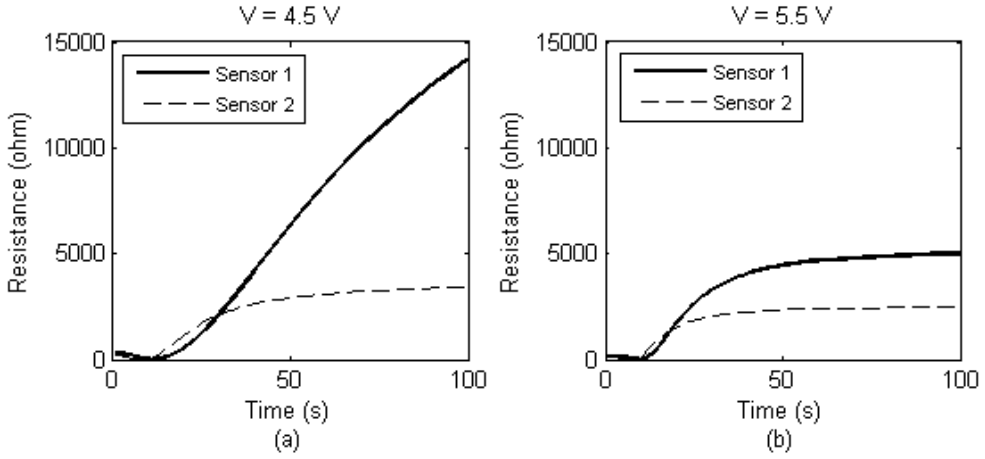

Figure 6.2 : Response of two sensors for acetaldehyde when heater voltage is (a) 4.5V and (b) 5.5V

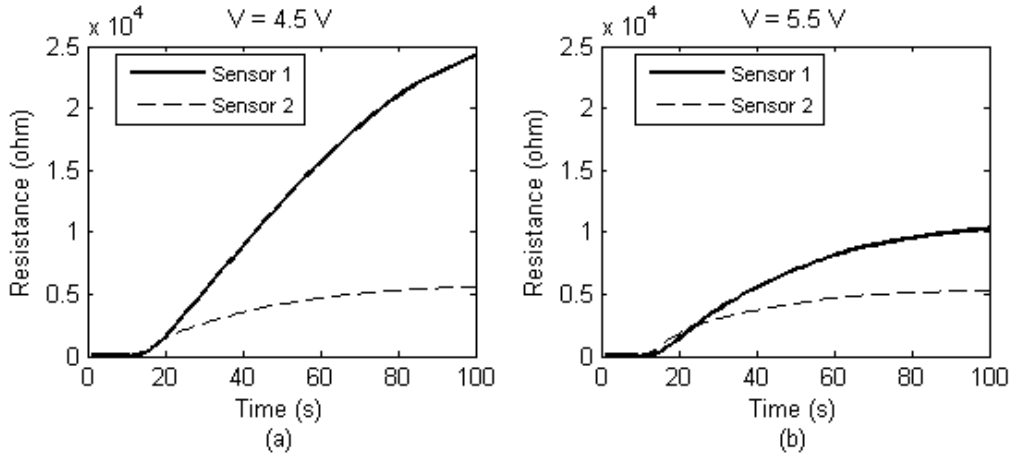

Figure 6.3 : Response of two sensors for acetone when heater voltage is (a) 4.5V and (b) 5.5V

Integrated data feature is generated by integrating the raw data from $t_0 = 0$ to **T**. The pattern at time **T** is

$$p_i(T) = \sum_{i=0}^{T} s_i(k) \qquad ,i = 1,2. \tag{6.1}$$

where s_i is the i^{th} sensor response.

Another feature is extracted regardless of time. The feature exponential moving average (EMA) is used for odor classification by Müezzinoğlu *et al* in [31]. EMA feature is actually a filtering process given with the transfer function

$$y_i(k) = (1-\alpha).y_i(k-1) + \alpha(s_{ii}(k) - s_i(k-1)) \qquad ,i = 1,2. \tag{6.2}$$

This feature is used to eliminate the time axis and revise the problem into another domain independent from time. However, another problem arises about optimization of the classification problem because a new parameter is introduced: α.

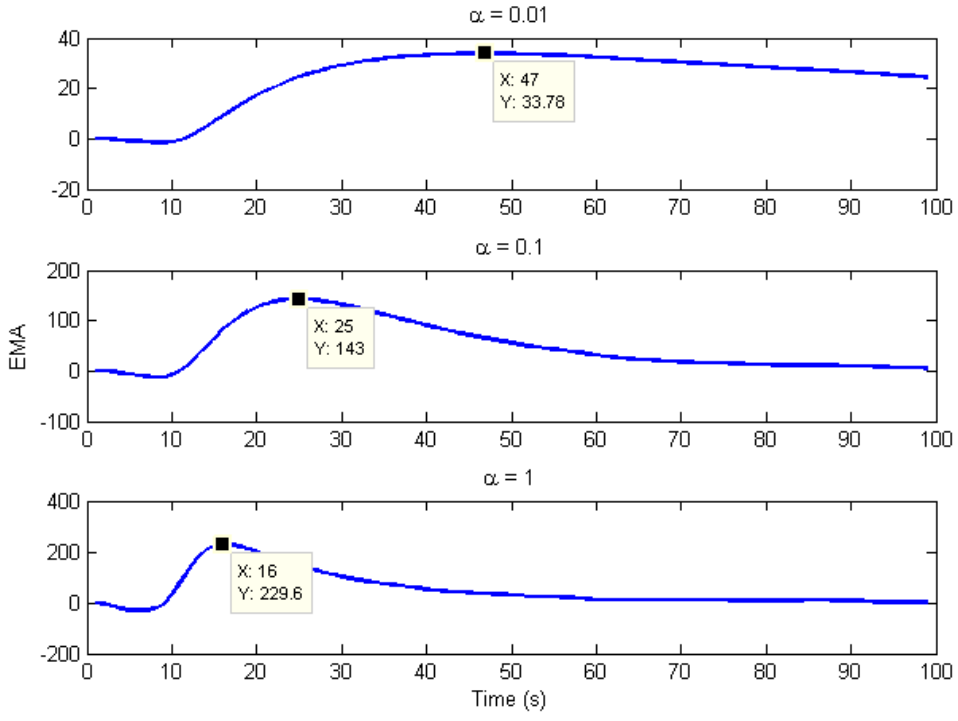

Figure 6.4 : EMA process for acetaldehyde when heater voltage is 5.5V.

Changing the α value changes the y_i function as given in Figure 6.4. α is scanned from 0.01 to 1 with steps of 0.01 and 100 two dimensional patterns are created by taking the maximum value of y_1 and y_2 calculated for the same α. Therefore, time is eliminated and patterns are generated as a function of α so classification process for EMA feature will be run at each α not at time snapshots. Search on α would not necessarily accelerate the classification due to the sensor recordings, but optimization on α is a required in this problem.

An example of EMA pattern versus α is given in Figure 6.5.

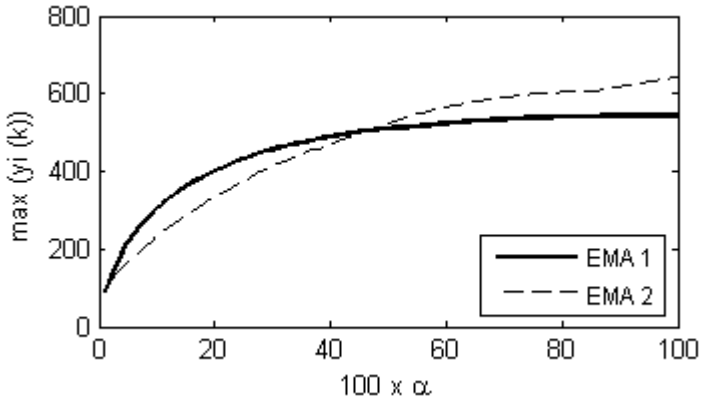

Figure 6.5 : EMA feature for Acetaldehyde when heater voltage is 5.5V.

6.3 Identification

Those patterns are used for identification and examined with four methods: Mutual Information (MI), One Nearest Neighborhood (1-NN), Naive Bayes Classifier (NBC) and Support Vector Machine (SVM).

In probability theory and information theory, the mutual information of two random variables is the mutual dependence of those two variables that is given without a unit. For each pattern generated in either of three ways introduced above, one of the random variable is the class of the pattern and the second variable comes from the sensory information. All the patterns involves two independent sensor information but they are represented as one variable in mutual information calculation.

The x-axis stands for the information from the first sensor and second one is placed in the y-axis in the coordinate plane. After the patterns are sketched on the coordinate plane, both of the axis are divided into four pieces equally forming 16 equal rectangles as shown in Figure 6.6.

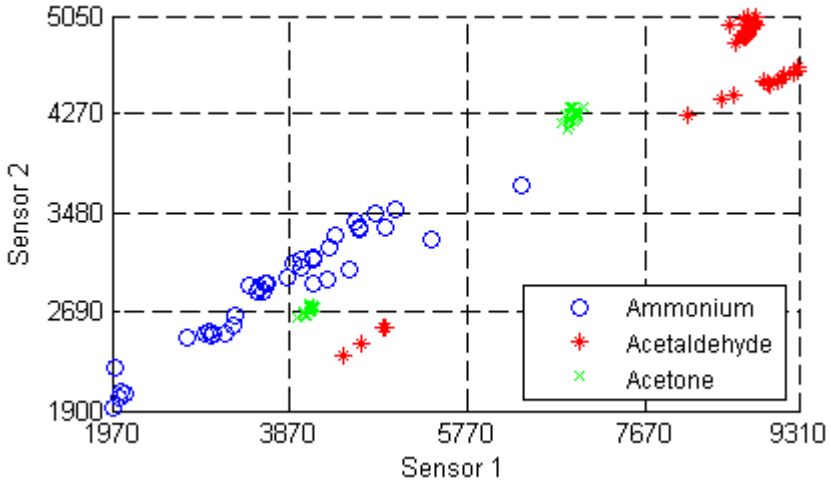

Figure 6.6 : Mutual Information calculation for raw data recorded at T=50s and 5.5V

Each pattern falls in one of those 16 bins and that bin is the second random varible. Then mutual information between the class and the bin of the pattern is calculated by

$$I(X,Y)=\sum_{y\in Y}\sum_{x\in X}p(x,y)\log\left(\frac{p(x,y)}{p_1(x)p_2(y)}\right) \qquad \textbf{(6.3)}$$

where random variable X is the bin and Y is the class; p(x,y) is joint probability distribution function of X and Y, $p_1(x)$ and $p_2(y)$ are the marginal probability distribution functions of X and Y respectively.

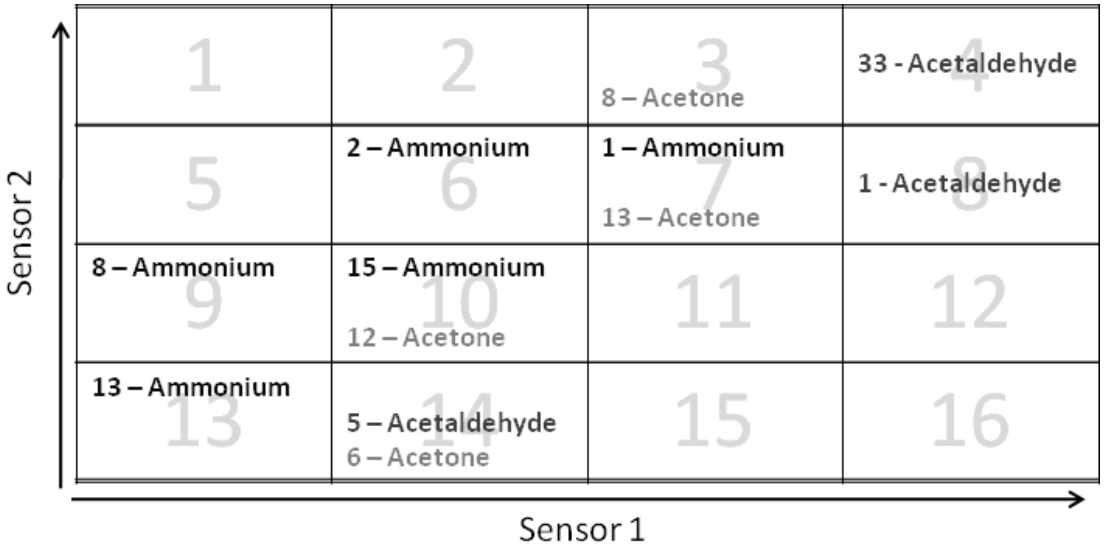

Figure 6.7 : Mutual information calculation step 1.

As an example, mutual information between sensory data and odor class is calculated for the set given in Figure 6.6. First of all, numbers of records are found in every bin as seen in Table 6.1.

Table 6.1 : Number ofodors belonging to specific class in the bins.

Class	Bin ID															
	1	2	3	4	5	6	7	8	9	10	11	12	13	14	15	16
Ammonium	0	0	0	0	0	2	1	0	8	15	0	0	13	0	0	0
Acetaldehyde	0	0	0	33	0	0	0	1	0	0	0	0	0	5	0	0
Acetone	0	0	8	0	0	0	13	0	0	12	0	0	0	6	0	0

Joint and marginal probability distribution functions can be found with the information given in Table 6.1, then mutual information is calculated using Equation (6.3) at this time snapshot.

Mutual information is not a quantity so it can only give an insight about the change in separability with altering heater voltage in time or α.

Mutual information is calculated at every time snapshot for eleven different heater voltages. In Figure 6.8, the highest mutual information obtained at time T is plotted in the lower graph. In Figure 6.8 (a), the heater voltage giving the highest mutual information at certain time snapshot is dotted. For example, at T=20 s, the highest mutual information is obtained with the data set recorded when heater voltage is 4.5V (from Figure 6.8 (a)) and the mutual information at this time is around 4.5 (Figure 6.8 (b)).

If the change of mutual information is investigated in time, the gap between 20th and 30th seconds should be explained. Referring to the Figure 6.1, this time interval is the change of slope for ammonium. Decrease in mutual information in this portion is a result of this sudden change in the sensor response. This fact will be investigated deeply for other classification tools.

Another representation is given in Figure 6.9, there mutual information is normalized to 1-100 where highest mutual information is given with 100 and represented with a color shown in the color map as darkest color is used for highest value. Three sketches belonging to three features can be seen in the figure: raw data, integrated data and EMA feature. x-axis of sketches for raw data and integrated data are time and it is α for EMA feature. The rows carry the heater voltage information. For example, mutual information change with time for the raw data record when heater voltage is set to 4.5V can be tracked in the top row of sketch 1. The darkest part of that row appears around T=45s, so the highest mutual information is gathered at 45^{th} second for this data set, if the heater voltage is 4.5V.

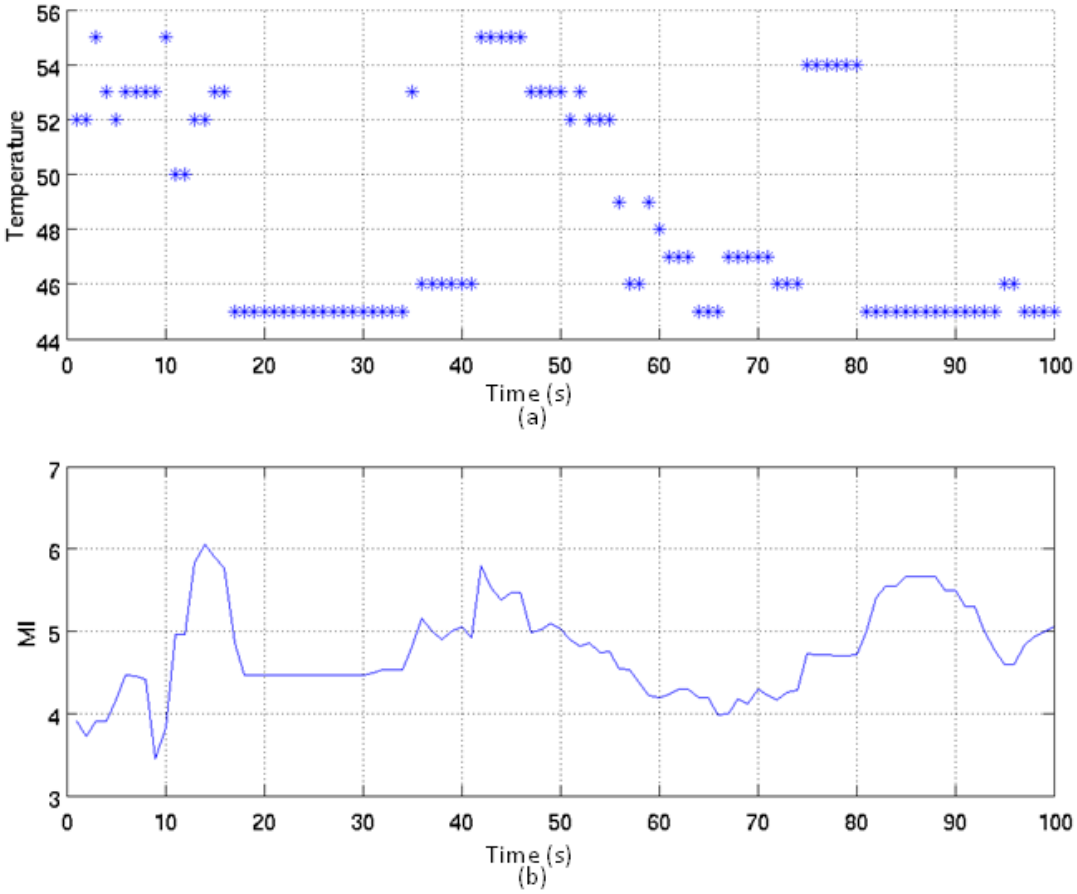

Figure 6.8 : Mutual information raw data.

For raw data feature, mutual information reaches its highest value for the first time when T=22 seconds for heater voltages of 5.2V or 5.3V. Therefore, if accelerating the classification in transient is the primary aim for this data set and feature, 5.2V and 5.3V are the optimum heater voltages.

Note that, characteristics change when the feature is changed to integrated data or EMA. Also, in EMA feature we cannot talk about the speed of records since we cannot be sure about when the moving average function will take its maximum value. Moreover if EMA feature is chosen to be used, sensor temperature should be set to 5.5 which draws the darkest row. In addition to mutual information, three classifiers are trained and tested as in memoryless case introduced in Section 5. Classifiers are validated with a technique similar to leave one out technique. For each time or α snapshot, two patterns are left for test and the classifier (1-NN, NBC or SVM) is trained with the remaining 115 examples. The performance of the classifier for every trial is recorded. Average of the recorded performances is considered as the performance of the classifier at that snapshot.

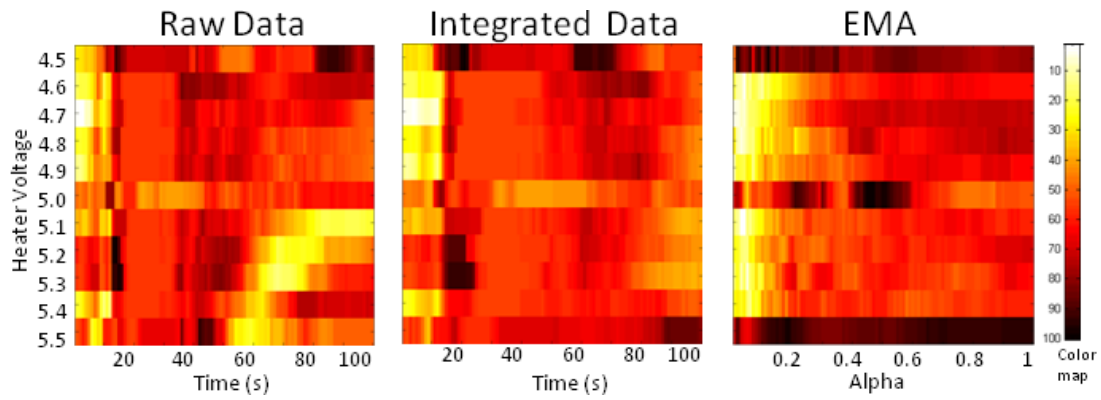

Figure 6.9 : Mutual information for each feature and heater voltages.

This procedure is repeated at every snapshot for those three features and eleven heater voltages. The performance of 1-NN is shown in Figure 6.10. The color map shows in performance in percent. The darkest color stands for the highest performance, 100%. It is visible that, there is a huge difference in performance between features. Although there is not much mutual information difference between data features and EMA feature, for this classifier the performance gathered with EMA feature is not satisfying. Moreover, the classification performance with integrated data is 100% after 50th second independent of heater voltage and high performances can be achieved before 20th second with integrated data feature when heater voltage is 5.5V.

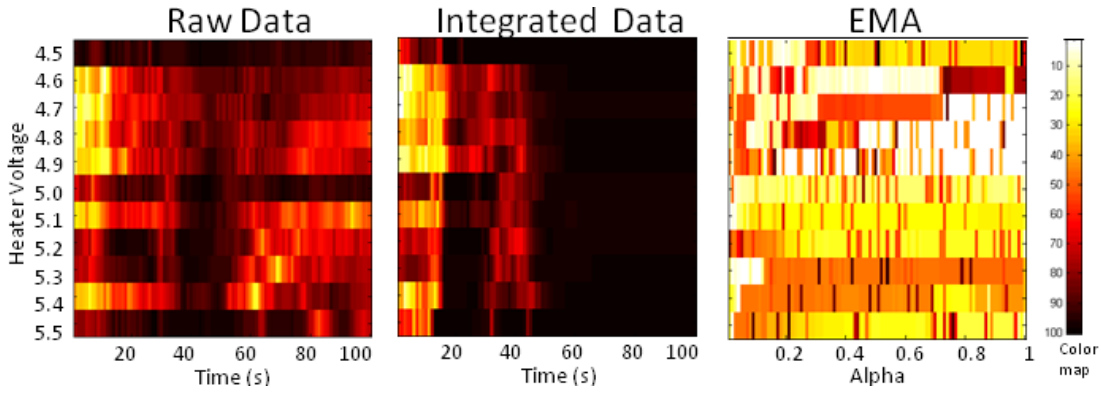

Figure 6.10 : Performance of 1-NN classifier for each feature and heater voltages.

In Figure 6.11, performance analysis with Naive Bayes Classifier is given. As in the 1-NN case, EMA feature does not give high scores. Moreover, the characteristic of integrated data after certain time is also similar. If this figure is examined with Figure 6.9, the similarity between color changes in data feature graphs can be cached especially around 20 seconds at 5.2V and 5.3V. The performance of SVM is extremely low and a smooth change cannot be observed with this graph.

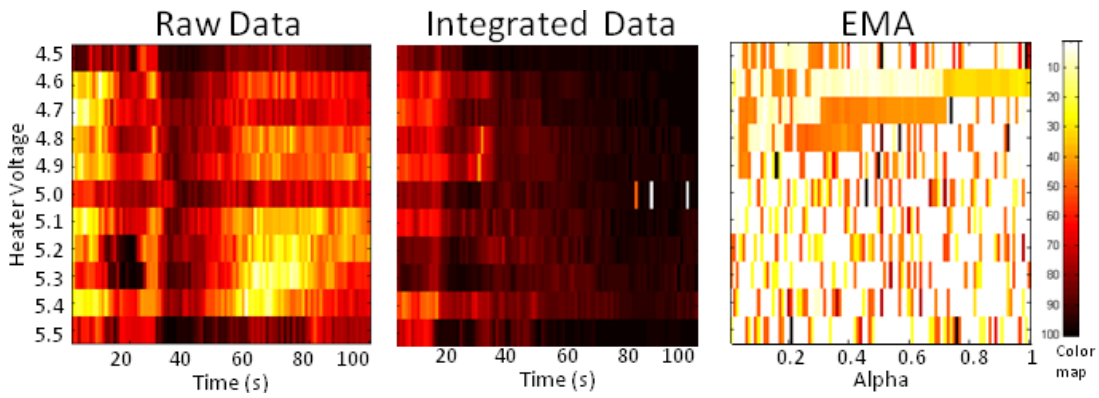

Figure 6.11 : Performance of NBC classifier for each feature and heater voltages.

Finally, the features are classified with SVM and results are given in Figure 6.12. The gap around 20-30 seconds which is shown in Figure 6.8 can be observed in the raw data and partially integrated data classification as light colors in Figure 6.12. Apart from previous classifiers, darkest graph is sketched for EMA feature. Darkest row of EMA feature is row of 5.5V as in mutual information case. Mutual information may give an insight about separability but as shown in these three classifiers, performance of classifiers does not always follow the mutual information.

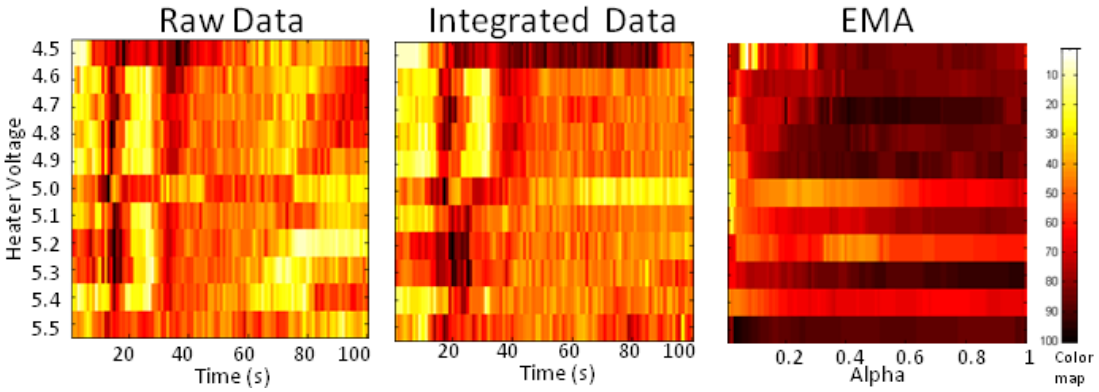

Figure 6.12 : Performance of SVM classifier for each feature and heater voltages.

6.4 Effect of Sensor Temperature on Two Layer CNN Based Model

A two layer having the template

$$A = \begin{bmatrix} A_{-1-1} & A_{-10} & A_{-11} \\ A_{0-1} & A_{00} & A_{00} \\ A_{1-1} & A_{10} & A_{11} \end{bmatrix} = \begin{bmatrix} 1 & 1 & 1 \\ 1 & 0 & 1 \\ 1 & 1 & 1 \end{bmatrix}$$

is driven by 16 metal oxide gas sensor response and output of each excitatory processors are collected.

Same as the previous CNN based artificial antennal lobe model tests, a pattern having the dimension of N_e is gathered at each time snapshot and those patterns are used as inputs of the classifier, SVM. The SVM is operated in memoryless case and validated with leave one out technique.

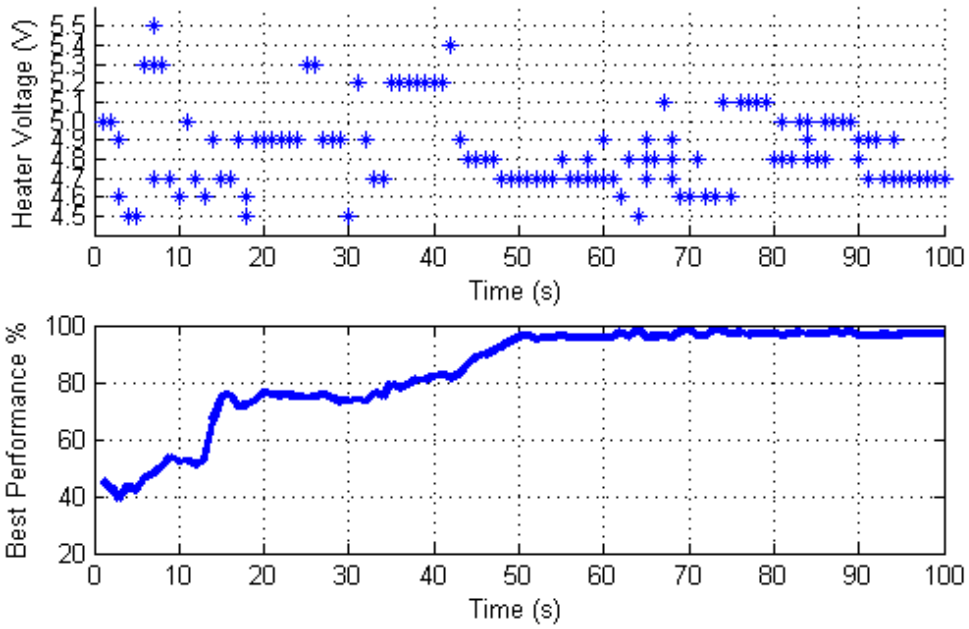

Figure 6.13 : Heater voltages giving the best performance for 2 layer CNN.

The best performance through heater voltages is recorded at each time snapshot as given in Figure 6.13. The performance of classifier exceeds 80% after 20th second when CNN feature is used with SVM classifier. Then performance reaches nearly 100% by time 50s. However, it is hard to give an optimum heater voltage for this problem, because the voltage value giving the best performance varies heavily in time. For example, after T=50 seconds, 4.7V gives the best performance for 10 seconds but then other heater voltages stars to give better classification results. Therefore, benefit of sensor temperature on classification performance is highly dependent on transient response.

7. CONCLUSION

In this thesis, a method to accelerate odor classification using the odor sensor response on transient rather than stable level is tried to be developed. The organ in insect olfaction system that converts spatial inputs to spatio-temporal patters, antennal lobe, is modeled with cellular neural networks. The collaboration of two types of neuron populations, which is the basis of spatio-temporal coding in the antennal lobe, is adapted to the cellular neural network which ordinarily include the cells having the same dynamics. Neuron populations are assumed to show a Wilson-Cowan like population dynamics. In order to protect the regularity of a CNN grid, two layer CNN is given where each layer is composed of the cells having the same dynamics. Therefore, the regularity of cell connections, the connection template, is preserved. The randomness of neuron connections in antennal lobe is presented to cellular neural networks with Small-World phenomenon. Benefit of the proposed models are tested with classification problems including different types of odor sets, one including two pure odors and mixtures of them and the other including five distinct odors. Both cases, use of CNN based antennal lobe models resulted in higher separability before obtaining a stable sensor response. For SWCNN, increasing the number of short-cuts did not increase the classification performance because regular CNN has the dynamics of a small world network since every cell is connected to each other directly or indirectly.

The effect of sensor temperature on classification is investigated with another three-class data set and not only the feature generated by CNN model but also three additional features are used as classifier input. The classification performance is highly depended on the data set, the feature extracted, the classifier type and the time window investigated in the transient. Therefore, a fixed optimum sensor temperature cannot be determined for classification.

Biological processes are fed from the collaboration of different neuron populations, so in order to use CNN in bio-inspired applications rather than human retina applications, distinct dynamics should be introduced in the same network. This thesis is one example for such an application.

This thesis demonstrates that, the proposed CNN based models show the dynamics of antennal lobe but in order to use the overall artificial olfaction system effectively, the parameters such as connection weights, cell numbers, gain and time constants should be optimized.

REFERENCES

[1] http://olfaction.ucr.edu/, accessed at 29.03.2010..

[2] **Pearce, T.C., and Schiffman S.S.,** 2003. Handbook of Machine Olfaction: Electronic Nose Technology, Wiley-VCH.

[3] General information for TGS sensors, http**://**www.figarosensor.com/products/common(1104).pdf accessed at 10.01.2010

[4] **Nef, P.,** 1998. How We Smell: The Molecular and Cellular Bases of Olfaction, *News in Physiological Sciences.*

[5] **Zarzo, M**., 2007. The sense of smell: molecular basis of odorant recognition, *Biological Reviews*.

[6] **Buck, L. and Axel, R.,** 1991. A novel multigene family may encode odorant receptors - a molecular-basis for odor recognition, *cell*, 65(1),pp. 175-187.

[7] American Society for Testing and Materials (ASTM), www.astm.org/, accessed at 10.01.2010

[8] **Gao, Q., Yuan, B. and Chess, A.,** 2000. Convergent projections of Drosophila olfactory neurons to specific glomeruli in the antennal lobe, *Nature Neuroscience*, 3(8), pp. 780-785.

[9] **Silbering, A.F. and Galizia, C.G.,** 2007. Processing of Odor Mixtures in the Drosophila Antennal Lobe Reveals both Global Inhibition and Glomerulus- Specific Interactions, *Journal of Neuroscience*, 27(44), pp. 11966-11977.

[10] **HANSSON, B.,** 1995. Olfaction in lepidoptera, E*xperıentıa*, 51(11), pp. 1003-1027**.**

[11] **Strausfeld, N., Hansen, L., Li, Y., Gomez, R. and Ito, K.,** 1998. Evolution, discovery, and interpretations of arthropod mushroom bodies, *Learning & Memory*, 5(1-2), pp. 11-37.

[12] **Zhou, W. and Chen, D.,** 2009. Binaral Rivalry between the Nostrils and in the Cortex, *Current Biology*, 19(18), pp. 1561-1565.

[13] **Morrison, E. and Costanzo, R.,** 1992. Morphology Of Olfactory Epıthelıum In Humans And Other Vertebrates, *Mıcroscopy Research And Technıque*, 23(1), pp. 49-61.

[14] **Persaud, K. and Dodd, G.,** 1982. Analysıs Ofdıscrımınatıon Mechanısms In The Mammalıanolfactory System Usıng A Model Nose, *Nature*, 299(5881), 352-355.

[15] http://www.figaro.co.jp/en/company3.html, accessed at 30.03.2010

[16] **Wilson, A.D. and Baietto, M.,** 2009. Applications and Advances in Electronic-Nose Technologies, *Sensors*, 9(7), pp. 5099-5148.

[17] **Winquist, F., Lundstrom, I. and Wide, P.,** 1999. The combination of an electronic tongue and an electronic nose, *Sensors And Actuators B-Chemical*, 58(1-3), pp. 512-517.

[18] **Gardner, J.W. and Bartlett, P.N.,** 2000. Electronic Noses. Principlesand Applications, *Measurement Science and Technology*, 11(7), p. 1087.

[19] **Albert, K., Lewis, N., Schauer, C., Sotzing, G., Stitzel, S., Vaid, T. and Walt, D.,** 2000. Cross-reactive chemical sensor arrays, *Chemical Reviews*, 100(7), pp. 2595-2626**.**

[20] **Demarne, V., Grısel, A., Sanjınes, R., Rosenfeld, D. And Levy, F.,** 1992. Electrıcal Transport-Propertıes Of Thin Polycrystallıne Sno2 Film Sensors, *Sensors And Actuators B-Chemıcal*, 7(1-3), pp. 704-708.

[21] **Strike, D., Meijerink, M. and Koudelka-Hep, M.,** 1999. Electronic noses - A mini-review, *Fresenıus Journal Of Analytıcal Chemıstry*, 364(6), pp. 499-505.

[22] **James, D., Scott, S., Ali, Z. and O'Hare, W.,** 2005. Chemical Sensors For Electronic Nose Systems, Microchimica Acta, 149(1-2), pp. 1-17.

[23] **Schaller, E., Bosset, J. and Escher, F.,** 1998. 'Electronic noses' and their application to food, *Food Science And Technology-Lebensmittel-Wissenschaft & Technologie*, 31(4), pp. 305-316.

[24] **Ampuero, S. and Bosset, J.O.,** 2003. The electronic nose applied to dairy products: a review, Sensors and Actuators B: Chemical, 94(1), pp. 1-12.

[25] **Hudon, G., Guy, C. and Hermia, J**., 2000. Measurement of odor intensity by an electronic nose, *Journal Of The Air & Waste Management Association*, 50(10), pp. 1750-1758.

[26] **Srivastava, A.K.,** 2003. Detection of volatile organic compounds (VOCs) using SnO2 gas-sensor array and artificial neural network, *Sensors and Actuators B: Chemical*, 96(1-2), pp. 24 - 37,

[27] **de Bruyne, M., Clyne, P.J. and Carlson, J.R.,** 1999. Odor coding in a model olfactory organ: The Drosophila maxillary palp, *Journal of Neuroscience*, 11, pp. 4520-4532.

[28] **Perez-Orive, J., Mazor, O., Turner, G.C., Cassenaer, S., Wilson, R.I. and Laurent, G.,** 2002. Oscillations and sparsening of odorrepresentations in the mushroom body, *Science*, 297, pp. 359-365.

[29] **Fernandez, P.C., Locatelli, F.F., Person-Rennell, N., Deleo,G. and Smith, B.H.,** 2009. Associative Conditioning Tunes Transient Dynamics of Early Olfactory Processing, *Journal of Neuroscience*, 29(33), pp. 10191-10202.

[30] **Phaisangittisagul, E.,** 2008. Transient Feature Extraction for Machine Olfaction based on Wavelet Decomposition, Proceedings Of The 2008 5th International Conference On Electrical Engineering Electronics, Computer, Telecommunications And Information Technology, Vols 1 And 2, Elect Engn, Elect, Comp,Telecommun & Informat Technol Asso c, IEEE, 345 E 47TH ST, NY 10017 USA, pp. 457-460.

[31] **Muezzinoglu, M.K., Vergara, A., Huerta, R., Nowotny, T., Rulkov, N., Abarbanel, H.D.I., Selverston, A.I. and Rabinovich, M.I**., 2009, Artificial Olfactory Brain for Mixture Identification., D. Koller, D. Schuurmans, Y. Bengio and L. Bottou, editors, *NIPS*, MIT Press, pp. 1121-1128.

[32] **Somboon, P., Wyszynski, B. and Nakamoto, T.,** 2007. Realization of recording a wide range of odor by utilizing both of transient and steady-state sensor responses in recording process, *SENSORS AND ACTUATORS B-CHEMICAL*, 124(2), pp. 557-563.

[33] **Phaisangittisagul, E. and Nagle, H.T.,** 2008. Sensor selection for machine olfaction based on transient feature extraction, *IEEE Transactions On Instrumentation And Measurement*, 57(2), pp. 369-378.

[34] **Phaisangittisagul, E., Nagle, H.T. and Areekul, V.,** 2010. Intelligent method for sensor subset selection for machine olfaction, *Sensors And Actuators B-Chemical*, 145(1), pp. 507-515.

[35] **WILSON, D. and DEWEERTH, S.,** 1995. Odor Discrimination Using Steady-State And Transient Characteristics Of Tin-Oxide *Sensors, Sensors And Actuators B-Chemical*, 28(2), 123-128.

[36] **Yamanaka, T., Ishida, H., Nakamoto, T. and Moriizumi, T**., 1998. Analysis of gas sensor transient response by visualizing instantaneous gas concentration using smoke, *Sensors And Actuators A-Physical*, 69(1), pp. 77-81.

[37] **Gutierrez-Osuna, R., Nagle, H. and Schiffman**, S., 1999. Transient response analysis of an electronic nose using multi-exponential models, *Sensors And Actuators B-Chemical*, 61(1-3), pp. 170-182.

[38] **Nakamoto, T., Iguchi, A. and Moriizumi, T.,** 2000. Vapor supply method in odor sensing system and analysis of transient sensor responses, *Sensors And Actuators B-Chemical*, 71(3), pp. 155-160.

[39] **Di Nucci, C., Fort, A., Rocchi, S., Tondi, L., Vignoli, V., Di Francesco, F. and Santos, M.**, 2003. A measurement system for odor classification based on the dynamic response of-OCM sensors, *IEEE Transactions On Instrumentation And Measurement*, 52(4), pp. 1079-1086, 19th IEEE Instrumentation and Measurement Technology Conference (IMTC/2002), Alaska, May 21-23, 2002.

[40] **Ishida, H., Nakayama, G., Nakamoto, T. and Moriizumi, T.,** 2005. Controlling a gas/odor plume-tracking robot based on transient responses of gas sensors, *IEEE Sensors Journal*, 5(3), pp. 537-545.

[41] **Jain, A., Duin, R. and Mao, J.**, 2000. Statistical pattern recognition: A review, *IEEE Transactions On Pattern Analysis And Machine Intelligence*, 22(1), pp. 4-37.

[42] **Ayhan, T., Muezzinoglu, M.K. and Yalcin, M.E.,** Feb. 3-5, 2010. Cellular Neural Network Based Artificial Antennal Lobe, in Proc.of the 12th IEEE International Workshop on Cellular Neural Networks and their Applications (CNNA 2010).

[43] **WILSON, H. and COWAN, J.,** 1972. Excitatory And Inhibitory Interactions In Localized Populations Of Model Neurons, *Biophysical Journal*, 12(1), pp. 1-37.

[44] **Chua, L.O. and Yang, L.,** 1988. Cellular neural networks: Theory and Applications, 35(10), pp. 1257-1290.

[45] **Yalçın, M. E.,** 2005. Cellular Neural Networks, Multi-Scroll Chaos and Synchronization, World Scientific.

[46] **ROSKA, T. and CHUA, L**., 1993. The Cnn Universal Machine - An Analogic Array Computer, *IEEE Transactions On Circuits And Systems Ii-Analog And Digital Signal Processing*, 40(3), pp. 163-173.

[47] **Rodriguez-Vazquez, A., Linan-Cembrano, G., Carranza, L., Roca-Moreno, E., Carmona-Galan, R., Jimenez-Garrido, F., Dominguez-Castro, R. and Meana, S.,** 2004. ACE16k: The third generation of mixed-signal SIMD-CNN ACE chips toward VSoCs, *IEEE Transactions On Circuits And Systems I-Regular Papers*, 51(5), pp. 851-863.

[48] **Watts, D. and Strogatz, S.,** 1998. Collective dynamics of 'small-world' networks, *Nature*, 393(6684), pp. 440-442.

[49] **HOPFIELD, J.,** 1982. Neural Networks Andphysical Systems With Emergent Collective Computational Abilities, Proceedings Of The National Academy Of Sciences Of The United States Of America-Biological Sciences, 79(8), pp. 2554-2558.

[50] **Bohland, J. and Minai, A.,** 2001. E-cient associative memory using small-world architecture, *NEUROCOMPUTING*, 38, pp. 489-496,

[51] **Zheng, P., Tang, W. and Zhang, J.,** 2010. A simple method for designing efficient small-world neural networks, *Neural Networks*, 23(2), pp. 155-159.

[52] **WHITE, J., SOUTHGATE, E., THOMSON, J. and BRENNER, S.,** 1986. The Structure Of The Nervous-System Of The Nematode Caenorhabditis-Elegans, *Philosophical Transactions Of The Royal Society Of London Series B-Biological Sciences*, 314(1165), pp. 1-340.

[53] **Yang, T. and Chua, L.,** 1999. Cellular neural networks can mimic small-world networks, *International Journal Of Bifurcation And Chaos*, 9(10), pp. 2105-2126.

[54] **Kazuya TSURUTA, Zonghuang YANG, Y.N. and USHIDA,** 2003, A. Small-World Cellular Neural Networks for Image Processing Applications, *Proceedings of European Conference on Circuit Theory and Design* (ECCTD'03).

[55] **Chang, C.C. and Lin, C.J.,** 2007. LIBSVM: a library for support vector machines, v2.85, software available at http://www.csie.ntu.edu.tw/ cjlin/libsvm.

[56] **Setkus, A., Olekas, A., Senuliene, D., Falasconi, M., Pardo, M. and Sberveglieri, G.,** 2009. Featuring Of Odor By Metal Oxide Sensor Response To Varying Gas Mixture, Pardo, M and Sberveglieri, G, editor, *Olfaction And Electronic Nose, Proceedings*, volume 1137 of AIP Conference Proceedings, pp. 202-205,

[57] **Wongchoosuk, C., Lutz, M. and Kerdcharoen, T.,** 2009. Detection and Classification of Human Body Odor Using an Electronic Nose, *SENSORS*, 9(9), pp. 7234-7249.

[58] **Campo, E., Ballester, J., Langlois, J., Dacremont, C. and Valentin, D.,** 2010. Comparison of conventional descriptive analysis and a citation frequency-based descriptive method for odor proling: An application to Burgundy Pinot noir wines, *Food Quality And Preference*, 21(1), pp. 44-55.

[59] **Wang, B., Xu, S. and Sun, D.W.,** 2010. Application of the electronic nose to the identification of different milk favorings, *Food Research International*, 43(1), pp. 255-262.

[60] **Pearson, K.,** 1901. On lines and planes of closest to systems of points in space, *Philosophical Magazine*, 2(6), pp. 559-572.

[61] **Jolliffe, I.T.,** 2002. Principal Component Analysis, Springer, 2nd edition,

[62] **CORTES, C. and VAPNIK, V.,** 1995. Support-Vector Networks, *Machine Learning*, 20(3), pp. 273-297.

[63] **Haykin, S.,** 1998. Neural Networks: A Comprehensive Foundation (2nd Edition), Prentice Hall, 2 edition,

[64] **Lee, A. and Reedy, B.,** 1999. Temperature modulation in semiconductor gas sensing, *Sensors And Actuators B-Chemical*, 60(1), pp. 35-42.

[65] **Gosangi, R. and Gutierrez-Osuna, R.,** 2010. Active Temperature Programming for Metal-Oxide Chemoresistors, *IEEE Sensors Journal*, 10(6), pp. 1075-1082.

[66] **Gutierrez-Osuna, R., Gutierrez-Galvez, A. and Powar, N.,** 2003. Transient response analysis for temperature-modulated chemoresistors, *Sensors And Actuators B-Chemical*, 93(1-3), pp. 57-66,

CURRICULUM VITA

Candidate's full name: **Tuba Ayhan**

Place and date of birth: **Ankara -26.01.1987**

Permanent Address: **İTÜ Elektrik Elektronik Fakültesi,**

Oda 1109, 34469, Maslak, İstanbul, Turkey

Universities and Colleges attended: **İstanbul Technical University, Elektronics Eng..**

Publications:

- **Ayhan T**., Müezzinoğlu M. K. and Yalcin M.E., "Cellular Neural Network Based Artificial Antennal Lobe," in *Proc.of the 12th IEEE International Workshop on Cellular Neural Networks and their Applications* (CNNA 2010), Berkeley, California, USA, Feb. 3-5, 2010, pp. 1-6.

- **Ayhan T**., Müezzinoğlu M. K. Vergara A. and Yalcin M.E., "Hücresel Yapay Sinir Ağı Tabanlı Olfaktif Bulb Modelinin Bir Koku Sınıflandırma Probleminde En İyi Sensör Sıcaklığın Bulunması İçin Kullanılması (Using A Cellular Neural Network Based Olfactory Bulb Model For Choosing the Best Sensor Temperature For An Odor Classification Problem)," *18. Sinyal İşleme Uygulamaları Kurultayı* (SIU 2010), Diyarbakır, Turkey, April 22-24, 2010, pp. 578-581 (In Turkish).

- **Ayhan T.,** Yalçın M. E., "FFT ALgoritmalarının FPGA Üzerinde Gerçeklenmesi", 1. Gömülü Sistemler ve Uygulamaları Sempozyumu (GÖMSİS 2008), İstanbul, 3-5 Kasım 2008. (In Turkish)